Energy Management in Grid-connected Microgrids with On-site Storage Devices

ENERGY MANAGEMENT IN GRID-CONNECTED MICROGRIDS WITH ON-SITE STORAGE DEVICES

BY

RAHELEH KHODABAKHSH, B.Sc.

A THESIS

SUBMITTED TO THE DEPARTMENT OF ELECTRICAL & COMPUTER ENGINEERING

AND THE SCHOOL OF GRADUATE STUDIES

OF MCMASTER UNIVERSITY

IN PARTIAL FULFILMENT OF THE REQUIREMENTS

FOR THE DEGREE OF

MASTER OF APPLIED SCIENCE

Master of Applied Science (2015) McMaster University
(Electrical & Computer Engineering) Hamilton, Ontario, Canada

TITLE: Energy Management in Grid-connected Microgrids with On-site Storage Devices

AUTHOR: Raheleh Khodabakhsh
B.Sc., (Electrical Engineering)
Isfahan University of Technology, Esfahan, Iran

SUPERVISOR: Dr. Shahin Sirouspour

NUMBER OF PAGES: xvi, 101

To my beloved husband:

Ali

Abstract

A growing need for clean and sustainable energy is causing a significant shift in the electricity generation paradigm. In the electricity system of the future, integration of renewable energy sources with smart grid technologies can lead to potentially huge economical and environmental benefits ranging from lesser dependency on fossil fuels and improved efficiency to greater reliability and eventually reduced cost of electricity. In this context, microgrids serve as one of the main components of smart grids with high penetration of renewable resources and modern control strategies.

This dissertation is concerned with developing optimal control strategies to manage an energy storage unit in a grid-connected microgrid under uncertainty of electricity demand and prices. Two methods are proposed based on the concept of rolling horizon control, where charge/discharge activities of the storage unit are determined by repeatedly solving an optimization problem over a moving control window. The predicted values of the microgrid net electricity demand and electricity prices over the control horizon are assumed uncertain. The first formulation of the control is based on the scenario-based stochastic conditional value at risk (CVaR) optimization, where the cost function includes electricity usage cost, battery operation costs, and grid signal smoothing objectives. Gaussian uncertainty is assumed in both net demand and electricity prices. The second formulation reduces the computations by taking a

worst-case CVaR stochastic optimization approach. In this case, the uncertainty in demand is still stochastic but the problem constraints are made robust with respect to price changes in a given range. The optimization problems are initially formulated as mixed integer linear programs (MILP), which are non-convex. Later, reformulations of the optimization problems into convex linear programs are presented, which are easier and faster to solve. Simulation results under different operation scenarios are presented to demonstrate the effectiveness of the proposed methods.

Finally, the energy management problem in network of grid-connected microgrids is investigated and a strategy is devised to allocate the resulting net savings/costs of operation of the microgrids to the individual microgrids. In the proposed approach, the energy management problem is formulated in a deterministic co-operative game theoretic framework for a group of connected microgrids as a single entity and the individual savings are distributed based on the Shapley value theory. Simulation results demonstrate that this co-operation leads to higher economical return for individual microgrids compared to the case where each of them is operating independently. Furthermore, this reduces the dependency of the microgrids on the utility grid by exchanging power locally.

Acknowledgements

Foremost, I would like to express my sincere gratitude and appreciation to my supervisor, Dr. Shahin Sirouspour for his patience, guidance, and supervision throughout this work. I would like to also thank my committee members, Dr. Nigel Schofield and Dr. James Chen for their interest in my work.

I take this opportunity to thank my fellow colleagues, Mohammad Jafarinasab, Adihithya Ravichandran, and Mohsen Rafiee for their help and encouragement throughout my masters at McMaster University.

I would especially like to thank my beloved husband for his constant caring, encouragement, understanding, and love. I deeply appreciate his support and would like to dedicate this work to him with all my love. Last but not the least, many thanks and appreciation to my parents for their endless love, sacrifice, and support throughout these years.

Notation and abbreviations

Notations and abbreviations:

CVaR - Conditional Value at Risk

DAB - Dual Active Bridge

DER - Distributed Energy Resources

DG - Distributed Generations

DLC - Direct Load Control

DSM - Demand-Side energy Management

EMS - Energy Management System

LP - Linear Program

MPC - Model Predictive Control

MILP - Mixed Integer Linear Program

RTP - Real-Time Pricing

ToUP - Time-of-Use Pricing

VaR - Value at Risk

Contents

List of Figures

Chapter 1

Introduction and Problem Statement

1.1 Motivation

In 2014, more than 67% of the electricity supply in the United States was generated by burning fossil fuels (i.e., coal, natural gas and petroleum) according to the US Energy Information Administration EIA [2014]. Although fossil fuels are considered to be inexpensive sources of energy, they are unsustainable and exploitation of such resources may lead to catastrophic effects on the earth climate and human health. Renewable energy sources such as wind and solar energy offer sensible and sustainable alternatives to fossil fuels. However, utilizing renewable energy sources poses its own challenges like finding suitable location for harvesting these sources and more importantly reliability concerns due to their intermittent nature. Reliability issues can partly be addressed by efficient integration of renewable resources with smart grid technologies.

Conventional power grid only permits a one-way flow of power from major electricity generators to consumers. However in recent years, a gradual transition to a smart grid environment has begun to allow for bi-directional flow of power between the grid and the end-users for better integration of clean sources of energy and storage capacity in the power system . Potential economical and environmental benefits arising for such model of grid operation are enormous, ranging from lesser dependency on fossil fuels, improved efficiency to greater reliability and eventually reduced cost of electricity.

As opposed to the centralized electricity generation paradigm in which electricity is produced in a large facility and transmitted to the consumers through long distribution networks, decentralized energy generation benefits from distributed energy generation in smaller scales. In this regard, microgrids with energy management system (EMS) can be considered as an effective platform for introducing distributed energy generation into the grid system.

A microgrid is a small electric grid system which could include a mixture of distributed energy sources (e.g., wind turbines, solar panels, fuel cells, and microturbines), loads (including controllable loads as HVAC unit) and storage devices (e.g., batteries, ultra-capacitors and flywheels) as well as a control unit. The control unit is responsible for operating the microgrid in an efficient way with the aim of reducing the cost of electricity for the consumer(s). It essentially determines charge/discharge activities of the storage devices, controls the HVAC unit, and may also help the grid with peak reduction, load shifting etc. Figure 1.1 depicts the main components of a grid-connected microgrid with EMS.

The intermittent nature of renewable energy sources stem from the fact that they

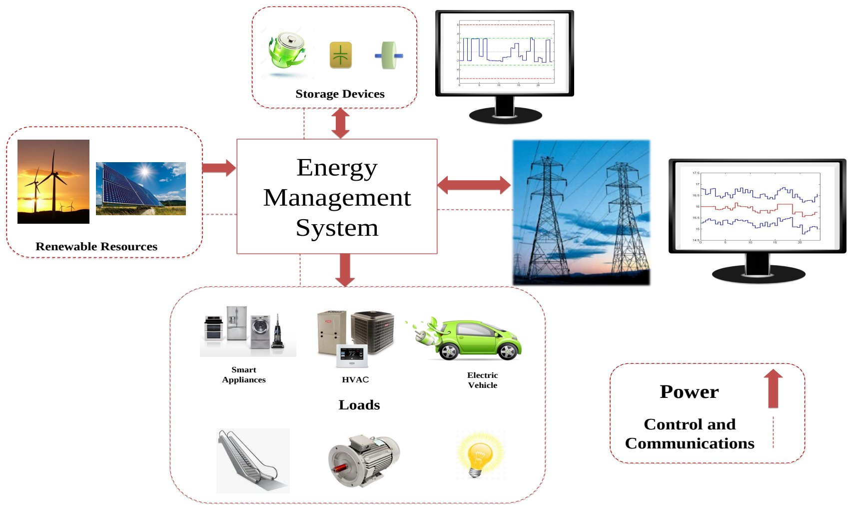

Figure 1.1: Schematic of a grid-connected microgrid with storage devices and Energy Management System

are not continuously available due to external factors like weather condition. The wind speed and sun radiations can vary significantly throughout day and night times resulting in large fluctuations in the output power of wind turbines and solar panels. On-site energy storage systems can be utilized to mitigate variations in the wind and solar power, by storing excess energy when available, and delivering it to the consumers when in demand. An energy management system can make optimal decisions with respect to charge/discharge of energy storage devices considering factors such as predicted energy demand, predicted energy generation from renewable sources, weather forecast, and electricity pricing. This can be achieved by formulating and solving relevant constrained multi-objective optimization problems, off-line or on-line.

There can be considerable uncertainty in the predicted values of demand, generation, and prices, and the solution obtained through optimization must be robust with respect to prediction errors. If unaccounted, these uncertainties may degrade the system performance. Our goal in this dissertation is to use modern optimization and modeling tools to design a controller that can efficiently operate a microgrid and account for the uncertainties in the system. The proposed controller performs as a high-level power optimizer in a hierarchical control structure. It provides power flow commands to a power converter device connecting the energy storage device to the microgird at a time scale in the order of minutes. A low-level power control system is also needed that would operate at a much faster time scale to enforce these power commands, and also handle voltage and frequency regulations, as required. A block diagram of the proposed controller is presented in a model predictive control (MPC) framework in Figure 1.2. It is noted that this thesis is only concerned with the high-level power scheduling control to ensure a certain degree of robustness to uncertainties in the net demand and electricity prices; the low-level control and protection system remains out of the scope of this dissertation.

Microgrids can gain access to greater local storage and energy resources through co-operations. Efficient co-operation of micro-grids increases the resiliency of the grid, would reduce power loss by using local resources and transmission lines, and decrease the dependency of local microgrids to the utility grid. In general, there is a limited storage capacity in microgrids which may not be sufficient to effectively deal with the fluctuations in their demand. Allowing local exchange of energy between individual microgrids may potentially compensate for the limited capacity, this reduce individual battery usage and prolong the life of the batteries.

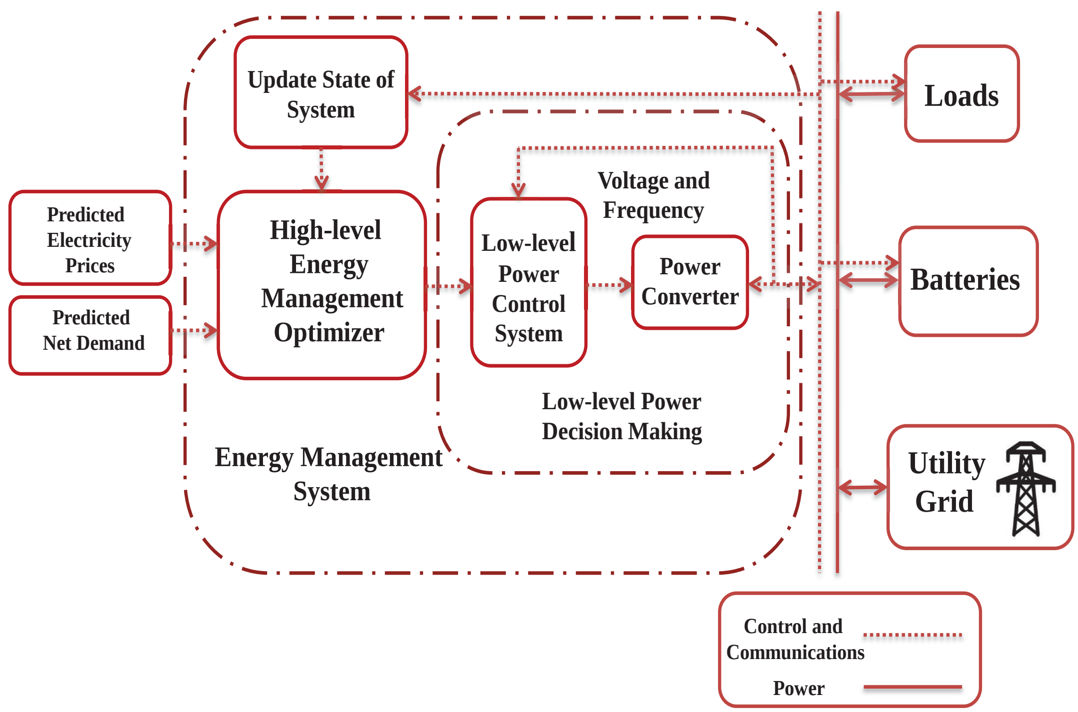

Figure 1.2: Block diagram of an MPC-based hierarchical energy management system

1.2 Problem Statement and Thesis Contributions

This thesis investigates the energy management problem for grid-connected micro-grids with batteries as on-site storage devices under presence of uncertainty in the electricity prices and predicted load and renewable power generation. In particular, solutions for the following problems are proposed:

- Optimal Energy Management under Uncertainty in Demand and Power Generated by Renewable Energy Sources

  The output power of renewable resources as well as the actual electricity usage of the loads are two of the system parameters which can be subject to uncertainty. In this work, a net demand vector is defined as the difference between the output power of the renewable resources and the electricity usage of the consumers. The primary concern here is to design a controller which is robust to variations of the net demand power. In particular, energy management problem is formulated as a mixed integer linear problem (MILP) as well as a linear problem (LP) within an on-line rolling horizon model predictive control framework. The uncertainty in the net demand vector is modeled as a Gaussian distribution around the predicted values and a stochastic scenario-based approach based on conditional value at risk (CVaR) minimization is proposed to make decisions which are robust to the uncertain variations of demand around its nominal values. The controllers decision vector consists of the rate by which batteries should either be charged or discharged.

- Optimal Energy Management with Joint Uncertainty in Demand and Electricity Prices

  Although, there are many cases in which electricity prices are known, specially for small-scale consumers, here we are looking at a future model of smart grid operation which allows market-based pricing of energy for small-scale consumers/producers of electricity. Electricity price forecasts are mainly based on statistical analysis of historical market prices. However, actual electricity market prices are influenced by many factors including demand and supply variations. Consequently, the actual prices may differ from the predicted values. In this problem, both demand and pricing signals are assumed to be uncertain and have independent variations around their nominal values. Two different approaches are proposed to formulate and solve the optimization problem under the presence of these uncertainties. The first method employs scenario-based minimization of CVaR of the cost, considering joint Gaussian uncertainty in the electricity demand and prices around their nominal predicted values. The resulting optimization problem in each step of the rolling horizon is of a MILP form. Furthermore, a reformulation of the energy management problem is proposed that avoids binary variables in a standard LP form.

The required number of sample scenarios to efficiently approximate the CVaR minimization problem grows exponentially in proportion to the number of uncertain parameters. In order to speed up the optimization, a second method is proposed in which scenario-based minimization only takes samples from net demand with Gaussian uncertainty. Electricity prices are assumed to vary within known bounds and this uncertainty is handled by worst-case robust approach. In particular, a reformulation of a constraint in CVaR minimization ensures that the worst-case cost with respect to price variations is considered in the optimization.

- Optimal Energy Management for Co-operative Microgrids with Renewable Energy Sources

  Co-operation of microgrids may result in higher economical return for the individual players by exploiting the fluctuations in demand as well as renewable energy. Furthermore, it reduces the dependency of the microgrids on the utility grid by exchanging power locally. In this thesis, a strategy is devised in order to allocate individual savings of a co-operative network of microgrids interconnected with the utility grid. In the proposed approach, the energy management problem is formulated in a deterministic co-operative game theoretic framework for a group of connected microgrids as a single entity and the individual savings are distributed based on the Shapley value (Roth [1988]).

1.3 Thesis Organization

The rest of this thesis is organized as follows. Chapter 2 reviews the literature on control strategies in energy management problem of microgrids. The energy management problem under uncertainty of electricity prices and net demand is formulated and solved by a scenario-based stochastic CVaR optimization in Chapter 3. Chapter 4 presents a less computationally expensive formulation of the problem by applying a Worst-Case CVaR approach. In order to demonstrate the effectiveness of the proposed methods, both chapters 3 and 4 are concluded with simulation results under different scenarios. Chapter 5 develops a LP formulation of the optimization problem for the proposed robust approaches introduced in chapter 3 and 4. This is followed by a multi-microgrid formulation of the problem in Chapter 6, where the energy management problem is solved in a co-operative game theoretic framework. The thesis is concluded in Chapter 7 where some possible directions for future work are discussed.

1.4 Related Publications

- R. Khodabakhsh and S. Sirouspour (2015, August). On-line Optimal Control of Energy Storage in a Microgrid by Minimizing Conditional Value-at-Risk. IEEE Transactions on Smart Grid (submitted).

Chapter 2

Literature Review

Microgrid control includes different aspects like managing distributed energy resources (DER) (such as micro turbine, wind turbine, fuel cell, and photovoltaic system), synchronization with the main utility grid, droop control, load and energy management, and optimizing the storage units. This chapter is divided into five sections. Section 2.1 provides a brief review on control strategies in microgrids including the DER management, synchronization with the main grid, and droop control. The rest of this chapter is concerned with the literature on storage units optimization and energy management of microgrids, which form the primary areas of the contributions of this thesis.

The energy management problem can be formulated and solved in two different scenarios. In the first one, electricity demand is assumed to be controllable, therefore, the controller seeks to reshape the demand signal to meet a certain set of criteria. However, in the second scenario, demand is assumed to be given and the controller governs the interactions between components of microgrid to compensate for the fluctuations in demand and minimize a global cost function. In this chapter, we refer to the first and second scenario as demand-side and utility-oriented energy management problem, respectively. In Section 2.2, we review the papers that study the demand-side energy management problem and Section 2.3 is devoted to utility-oriented studies. Section 2.4 also investigates different methodologies employed to address the energy management problem. These include off-line, on-line model predictive control, robust, and stochastic approaches. Finally, a brief literature review on relevant control strategies in multi-microgrid energy management problem is provided in Section 2.5.

2.1 A General Overview on Microgrid Control Strategies

Optimal control of DER can potentially improve the grid reliability and provide differentiated services to the customers. Mehrizi-Sani and Iravani [2010] introduced a method for controlling DER units of microgrids in both islanded and grid-connected modes based on the potential functions concept. The controller minimizes the potential functions associated with DER units based on a gradient decent method in a discreet-time manner and the control goal of each unit is obtained at the minimum of its corresponding potential function. Logenthiran et al. [2008] developed an agent-based model for optimal control of DER in AC microgrids by using the JAVA Agent Development (JADE) framework. A decentralized control strategy for optimal operation of microgrids with multiple DER units in autonomous mode is provided in Etemadi et al. [2012]. The proposed control scheme provides power management of the microgrid, frequency control, and local control of the DER units.

Voltage and frequency droop control enables efficient power sharing along with voltage regulation in microgrids with multiple distributed generations (DG). Droop control strategies are studied in both islanded and grid-connected operating modes of microgrids (e.g., see Mohamed and El-Saadany [2008], Majumder et al. [2009], Sao and Lehn [2008], Kim et al. [2011], Shafiee et al. [2014]). In Kim et al. [2011], a mode adaptive microgrid control strategy based on droop control is proposed for optimal management of power flow between microgrid converters in a decentralized manner. The proposed control scheme enables a smooth transition between the operation modes of the microgrid by using integral and derivative controllers in grid-connected and islanded modes, respectively. Shafiee et al. [2014] presented a distributed control strategy in droop-controlled microgrids including frequency, voltage, and reactive power sharing controllers. The proposed decentralized controller aims at removing voltage and frequency steady state errors along with optimal reactive power sharing between DG units.

In Rekik et al. [2015], a synchronization technique is presented for interconnecting a microgrid including wind turbine generators to an electrical network. The proposed method ensures a smooth reconnection to the utility grid with considering the fluctuations in renewable output power and demand. The synchronization is carried out in a grid-connected power converter which regulates and adapts the magnitude, frequency and phase of the microgrid voltage to those of the main grid.

2.2 Demand-Side Energy Management Studies

Load management also referred to as demand-side energy management (DSM) dates back to the early 1980s (Gellings [1985]) and has received significant interest in both research and industry. DSM programs offered by utility companies allow energy users to gain revenue by adjusting their demand in favor of the energy providers. This way, grid stability is maintained through demand adjustment rather than manipulating the supplied energy. DSM programs have been investigated in residential or commercial load management with the aim of reshaping consumers' consumption pattern (e.g., see Gottwalt et al. [2011], Mohsenian-Rad et al. [2010a,b]). Direct load control (DLC) and smart pricing are two popular techniques employed in residential load management.

In DLC programs, a mutual agreement grants the right to the utility company to remotely control the energy consumption of the consumers (Ruiz et al. [2009], Gomes et al. [2007], Weers and Shamsedin [1987]). However, concerns regarding privacy issues of DLC programs make them less attractive in practice. On the other hand, smart pricing programs intend to encourage the consumers to reduce their electricity demand by providing real-time pricing (RTP) and time-of-use pricing (ToUP) tariffs (Herter [2007], Triki and Violi [2009], Chen et al. [2010], Mohsenian-Rad et al. [2010a]). (Triki and Violi [2009]) proposed a dynamic retail tariff structure for utility companies by applying stochastic programming. (Chen et al. [2010]) utilized two market models to shape and design demand response while maintaining the balance with supply at all times. Their objective is to find a compromise between the costs and utilities among customers as well as the costs and utilities over time. This can motivate customers to shift their usage to off-peak periods which eventually reshapes the demand profile to flatter form. (Mohsenian-Rad et al. [2010a]) developed a game-theoretic approach to solve the demand-side energy management problem of residential settings by providing a simple pricing mechanism. In the proposed approach, users who share the same energy source are the game players and their objective is to minimize the individual electricity cost. The optimal solution is obtained at the

Nash equilibrium of the formulated problem and reduces the peak-to-average ratio in total demand as well as the total energy cost.

2.3 Utility-Oriented Optimization Studies

Unlike the DSM programs, utility-oriented methodologies intend to optimize a utility or cost function by controlling the elements in microgrids (e.g., batteries, Electric Vehicles, and controllable loads) given the demand data as model parameters. Storage devices increase the flexibility and reliability of the microgrids by compensating for the factors that impose uncertainties on the system including intermittent energy sources, variability of electricity prices, and consumers' demand. (Levron et al. [2013]) proposed an algorithm to address the energy management problem by considering the limitations imposed by storage devices including power, voltage, and current constraints. In (Mohamed and Koivo [2007], Hafez and Bhattacharya [2012]), a multi-objective optimization problem is employed to model the energy management of microgrids consisting of batteries as storage devices, which aims at reducing the emissions and operating cost of the microgirds. In (Zhou et al. [2011]), an algorithm is introduced for the control of a hybrid ultacapacitor-battery as storage device. It is argued that this combination could yield a high-power and high-energy storage system that can improve microgrid efficiency and reduce its net energy cost. The proposed algorithm deploys bidirectional dual active bridge (DAB) converters to assign steady and transient power demand to the batteries and the ultracapacitors, respectively.

2.4 Energy Management Techniques

The works in the energy management literature can also be categorized based on their approach for formulating and solving the problem. Off-line approaches have been extensively studied in EMS (Handschin et al. [2006], Deng et al. [2011], Levron et al. [2013]). Such approaches are mainly based on the assumption of availability of data at the moment of decision. However, due to the uncertain nature of the microgrids including renewable sources, this type of assumptions lead to inefficient decisions. Although there have been efforts to account for uncertainties and disturbances using off-line robust and stochastic optimization techniques, e.g. see Handschin et al. [2006], Chaouachi et al. [2013], Mohammadi et al. [2013], lack of feedback from the actual system can substantially limit the performance of such techniques. In addition to off-line optimization-based approaches, on-line MPC or rolling horizon control approaches have also been studied in the EMS literature (Peters et al. [2011], Zong et al. [2012], Hooshmand et al. [2012], Prodan and Zio [2014], Bruni et al. [2015], Silvente et al. [2015]). These methods benefit from the feedback mechanism of the controller to compensate for the system prediction errors including demand and energy market prices. In (Parisio and Glielmo [2011]), an online MPC-based control strategy is developed to solve the energy management problem by assuming availability of precise information on microgrid state as well as future loads of the system.

Online optimization-based MPC techniques rely on solving a real-time optimization problem. The system parameters of the underlying optimization model are highly exposed to uncertainty due to the intermittent nature of renewable energy sources, consumers' demand as well as variations in electricity market prices. Consequently, disregarding these uncertainties may cause the problem to become infeasible or the solution to be sub-optimal (Ben-Tal and Nemirovski [2000]). Several probabilistic and non-probabilistic approaches have been proposed to account for such uncertainties in the energy management problem. A robust optimization approach for modeling the uncertainty in the net demand of microgrids with storage devices and renewable energy sources is proposed in (Malysz et al. [2014]). The model solves a worst-case robust optimization which is subject to a box uncertainty around the predicted values of the consumers' demand. In (Zhang et al. [2012]), the energy management problem of a grid-connected microgrid is addressed considering the worst-case transaction cost induced by the uncertainty of renewable resources.

Although worst-case robust optimization provides a simple framework to deal with the optimization problems under uncertainty, over-conservatism and risk aversion makes it less attractive in practical applications (Thiele [2010]). Conditional Value at Risk (CVaR), introduced by Rockafellar and Uryasev (Rockafellar and Uryasev [2000]), is a coherent risk measure and has been widely used in finance and portfolio optimization (Fabozzi et al. [2007]). Unlike the conventional robust optimization approaches, CVaR-based optimization provides more flexibility by using the distributional information on the system uncertain parameters. In fact, CVaR minimizes the risk of the system being exposed to high losses rather than minimizing the worst-case cost. Recently, CVaR has been applied to energy management problem of microgrids as a risk-aware stochastic approach to account for system uncertainties (Zhang and Giannakis [2013], Wu et al. [2014], Siddiqui [2010]). (Zhang and Giannakis [2013]) formulated a stochastic optimization problem with a CVaR-based regularizer in microgrids with highly penetration of wind turbines. A CVaR-based real-time scheduling of residential appliances including air conditioner, hair dryer, electric vehicle and batteries has been studied in (Wu et al. [2014]).

2.5 A Brief Review on Management of Multi-Microgrids Systems

Several centralized approaches have been investigated in power flow problem of multiple distribution networks (Bruno et al. [2011], Paudyal et al. [2011]). However, the resulting centralized solutions suffer from scalability (Bruno et al. [2011]) and privacy issues (Paudyal et al. [2011]) which makes them unattractive. Alternatively, decentralized techniques have been proposed to address the power flow problem in distributed networks (Colson and Nehrir [2011], Nguyen and Le [2013]). (Colson and Nehrir [2011]) developed a real-time decentralized multi-agent controller for optimal management of available resources in a multi-microgrid system. In the proposed model, agents assigned to the microgrids are authorized to make decisions independently to achieve user-defined local objectives. In the meantime, they have the capability to co-operate together to pursue their common goals and reduce their dependency on the utility grid. (Nguyen and Le [2013]) proposed an optimal energy management co-operative framework for a group of interconnected microgrids. The proposed model employs a scenario-based two-state stochastic optimization approach to tackle the system uncertainty associated with renewable energy generation.

Game theoretic methods have been extensively applied to address the energy management problem of a group of microgrids(Alam et al. [2013], Chakraborty et al. [2015]). (Chakraborty et al. [2015]) presented an on-line strategy for exchanging energy in co-operative microgrids by proposing a coalition formation method. The proposed method benefits from a hierarchical priority based coalition scheme (HRCoalition) to minimize the power loss and dependency on the utility grid and at the same time maximize the power transfer within the microgrids in coalition. (Alam et al. [2013]) presented a coalitional model of energy exchange in a group of interconnected residential settings equipped with batteries and wind turbines or solar panels as microgeneration units. The proposed model benefits from Shapley Value and simulation results indicate significant reduction in battery as well as energy cost. However, their model does not consider utility oriented goals related to grid and battery signal shaping features.

Chapter 3

A CVaR-based Control Strategy in Energy Management of Microgrids

This chapter studies the control of batteries as storage units in a grid-connected microgrid with explicit consideration of uncertainty in the formulation of the optimization problem. In this problem, both electricity demand and prices are assumed to be uncertain and have independent variations around their nominal values. The goal here is to design a robust controller that can efficiently manage the batteries and account for such uncertainties in the system. In this regard, a stochastic scenario-based approach based on CVaR minimization is proposed to ensure a certain degree of robustness to the fluctuations of electricity demand and prices around their nominal values. The proposed method is based on the concept of rolling horizon control, where battery charge/discharge activities are determined by repeatedly solving a MILP optimization problem over a moving control window.

This chapter is divided into four sections. A non-robust MILP optimization formulation of the problem is presented in Section 3.1. This is followed by a brief introduction on CVaR in Section 3.2. Moreover, a robust formulation of the problem based on CVaR minimization is proposed in Section 3.3. Simulation results under different scenarios are presented in Section 3.4 to evaluate and compare performance of the proposed robust approach to its non-robust counterpart.

3.1 Non-robust Formulation

The non-robust formulation presented in this section is mainly based on the work in Malysz et al. [2014] and constitutes a reference for comparison with the robust approaches proposed in this dissertation. The non-robust formulation is based on the assumption that microgrid net demand power, i.e., the difference between the user demand and power from renewable sources, as well as the market price of electricity are precisely predicted. This work is not concerned with the prediction algorithm and assumes the predicted data are available as inputs to the controller. Although this thesis assumes battery for energy storage, its results could be easily extended to other types of storage devices. A similar discrete-time battery model as in Malysz et al. [2014] is employed in which two different modes of battery operation are considered. In its green zone rates, the battery can operate safely for an arbitrary long period of time, whereas in its red zone, the battery can temporarily increase its charge/discharge rates over their normal limits for a short period of time. The controller essentially determines the rates by which the battery should be charged or discharged. The goal is to minimize the cost of electricity, ensure smoothness of the power profile at the point of common coupling to the grid, reduce battery operating cost, while supplying the user power demand.

In this work, the control values are optimized considering the following cost function associated with the decisions and system parameters,

$$\begin{aligned} J \triangleq\, & c_{batg}^T p_{bat}^{gc} + c_{batg}^T p_{bat}^{gd} + c_{batr}^T p_{bat}^{rc} + c_{batr}^T p_{bat}^{rd} \quad (a) \\ & + c_{smg}^T u_g + c_{smb}^T u_b \quad (b) \\ & + c_{peak} p_g^{ob} + c_{flat}(p_g^{max} - p_g^{min}) \quad (c) \\ & + C_E \quad (d). \end{aligned} \tag{3.1}$$

The sum of the terms in (a) represents the cost associated with operating the batteries in green or red zone. Here, p_{bat}^{gc} and p_{bat}^{gd} are the green zone power rates for charging and discharging the batteries and c_{batg} is the associated cost. Similarly, p_{bat}^{rc} and p_{bat}^{rd} represent red zone charging and discharging power rates, and c_{batr} is its corresponding cost. The term (b) penalizes the grid and battery signal non-smoothness where, u_b and u_g represent magnitude of the variations in battery and grid power rates in consecutive horizon time-steps. The first term in (c) reduces the peak in demand at point of common coupling by penalizing excess demand p_g^{ob} over a baseline power rate p_g^{base} set by the user (see Malysz et al. [2014] for details). The second term flattens the grid power signal p_g by penalizing the difference between its maximum and minimum values. The last term in (d) also represents the cost of electricity bought/sold from/to the utility grid and is defined as follows

$$C_E = c_{buy}^T p_b + c_{sell}^T p_s, \tag{3.2}$$

where c_{buy} and c_{sell} represent the electricity buying and selling prices, and p_b and p_s are time-averaged energy bought or sold, respectively. They are defined as

$$p_b \triangleq \max\left(p_d + p_{bat}^{gc} + p_{bat}^{rc} - p_{bat}^{gd} - p_{bat}^{rd}, 0\right), \tag{3.3}$$

$$\begin{aligned} p_s &\triangleq \min\left(p_d + p_{bat}^{gc} + p_{bat}^{rc} - p_{bat}^{gd} - p_{bat}^{rd}, 0\right) \\ &= p_d + p_{bat}^{gc} + p_{bat}^{rc} - p_{bat}^{gd} - p_{bat}^{rd} - p_b. \end{aligned} \tag{3.4}$$

Substituting (3.4) in (3.2) yields

$$\begin{aligned} C_E &= (c_{buy}^T - c_{sell}^T)p_b \\ &\quad + c_{sell}^T(p_d + p_{bat}^{gc} + p_{bat}^{rc} - p_{bat}^{gd} - p_{bat}^{rd}). \end{aligned} \tag{3.5}$$

Assuming $c_{buy} \geq c_{sel}$, the nonlinearity introduced in the cost by the max function in (3.3) can be eliminated using the following constraints

$$\begin{aligned} &p_b \geq p_d + p_{bat}^{gc} + p_{bat}^{rc} - p_{bat}^{gd} - p_{bat}^{rd}, \\ &p_b \geq 0. \end{aligned} \tag{3.6}$$

Substituting (3.5) in the loss function introduced in (3.1) results in the following optimization problem

$$\begin{aligned}
\min \quad & (c_{batg}^T p_{bat}^{gc} + c_{batg}^T p_{bat}^{gd} + c_{batr}^T p_{bat}^{rc} + c_{batr}^T p_{bat}^{rd} \\
& + c_{smg}^T u_g + c_{smb}^T u_b \\
& + c_{peak} p_g^{ob} + c_{flat}(p_g^{max} - p_g^{min}) \\
& + (c_{buy}^T - c_{sell}^T) p_b + c_{sell}^T (p_d + p_{bat}^{gc} + p_{bat}^{rc} - p_{bat}^{gd} - p_{bat}^{rd})) \qquad (3.7)
\end{aligned}$$

subject to:

$$\begin{aligned}
& p_b \geq p_d + p_{bat}^{gc} + p_{bat}^{rc} - p_{bat}^{gd} - p_{bat}^{rd}, \\
& p_b \geq 0.
\end{aligned}$$

The following subsection introduces additional constraints which are imposed by limits on battery power/energy and grid power signal(Malysz et al. [2014]).

3.1.1 Additional Constraints

In this work, a discrete-time model for battery storage devices is employed as follows

$$E_{k+1} = E_k + \eta_c h_k p_{batk}^c - \eta_d^{-1} h_k p_{batk}^d - P_{bat}^{loss} h_k, \qquad (3.8)$$

where E_k represents the energy of battery at time step k in kWh, h_k is the length of the time step measured in hours, P_{bat}^{loss} is the self discharging power of the battery in kW per hour, p_{bat}^c and p_{bat}^d, η_c, and η_d represent battery charging and discharging power and efficiency, respectively. The following inequality constraint ensures that the battery energy level remains within safe limits at each time step,

$$\begin{aligned} E_{bat}^{min} \leq \eta_c \sum_{i=1}^{k} h_i(p_{bat_i}^{gc} + p_{bat_i}^{rc}) - p_{bat}^{loss} \sum_{i=1}^{k} h_i \\ -\eta_d^{-1} \sum_{i=1}^{k} h_i(p_{bat_i}^{gd} + p_{ba}^{rd}) + E_{bat}^{0} \leq E_{bat}^{max} \quad \text{for} \quad k \in [1, Nh], \end{aligned} \tag{3.9}$$

where E_{bat}^{0} is battery energy level at the beginning of the control horizon, and E_{bat}^{min} and E_{bat}^{max} denote minimum and maximum allowable battery energy levels.

Battery charging/discharging powers are also constrained through the following constraints

$$\begin{aligned} &0 \leq p_{bat}^{gc} \leq p_{bat}^{gc,max} \delta_{cd} \\ &0 \leq p_{bat}^{rc} \leq p_{bat}^{rc,max} \delta_{cd} \\ &0 \leq p_{bat}^{gd} \leq p_{bat}^{gd,max} (1 - \delta_{cd}) \\ &0 \leq p_{bat}^{rd} \leq p_{bat}^{rd,max} (1 - \delta_{cd}) \\ &0 \leq p_{bat}^{rc} \leq p_{bat}^{rc,max} \delta_{r} \\ &0 \leq p_{bat}^{rd} \leq p_{bat}^{rd,max} \delta_{r}, \end{aligned} \tag{3.10}$$

where the scalar constants $p_{bat}^{gc,max}, p_{bat}^{gd,max}, p_{bat}^{rc,max}, p_{bat}^{rd,max}$ represent the maximum battery charging and discharging rate in the green and red zones, respectively. Moreover, δ_{cd}, δ_r are binary vectors of length N_h which indicate the state of the batteries at each time step (i.e., charging/discharging and green/red zone operation). Furthermore, to make sure that the green zone rates are used first we should have

$$\begin{aligned} &p_{bat}^{gc,max} \delta_r - p_{bat}^{gc,max} (1 - \delta_{cd}) \leq p_{bat}^{gc}, \\ &p_{bat}^{gd,max} \delta_r - p_{bat}^{gd,max} \delta_{cd} \leq p_{bat}^{gd}. \end{aligned} \tag{3.11}$$

For safety reasons, red-zone power rates can be only activated for a maximum time of T_{max}^{on}, after which a minimum cool down time of T_{min}^{off} is needed before red-zone rates could be used again. The constraints concerning these maximum on-time and minimum off-time are presented in the following

$$\sum_{k=j}^{j+T_{max_j}^{on}} h_k \delta_{rk} \leq T_{max}^{on} \quad \forall j \in [j_{min}, j_{max}] \tag{3.12}$$

$$j_{min} = 2 - min_{h_1 l > T_{max}^{on}} l \in \mathcal{Z} \tag{3.13}$$

$$j_{max} = max_{\sum_{k=\gamma}^{N_h} h_k > T_{max}^{on}} \gamma \in \mathcal{Z} \tag{3.14}$$

$$T_{max_j}^{on} = min_{\sum_{k=j}^{j+\tau} h_k > T_{max}^{on}} \tau \in \mathcal{Z} \tag{3.15}$$

$$\begin{aligned} &\delta_{r_{j-k-1}} - \delta_{r_{j-k}} \leq 1 - \delta_{r_j} \\ &\forall k \in [1, T_{min_j}^{off} - 1], \forall j \in \{[1, Nh] | T_{min_j}^{off} \geq 2\} \end{aligned} \tag{3.16}$$

$$T_{min_j}^{off} = min_{\sum_{k=j-r}^{j-1} h_k \geq T_{min}^{off}} \tau \in \mathcal{Z}, \ \tau \geq 1 \tag{3.17}$$

The battery signal smoothness is also imposed by the following constraint

$$\begin{aligned} &-\Delta p_{bat} h \leq -u_{b_k} \leq p_{bat_k}^{gc} + p_{bat_k}^{rc} - p_{bat_k}^{gd} - p_{bat_k}^{rd} \\ &- p_{bat_{k-1}}^{gc} - p_{bat_{k-1}}^{rc} + p_{bat_{k-1}}^{gd} + p_{bat_{k-1}}^{rd} \leq u_{b_k} \leq \Delta p_{bat} h \end{aligned} \tag{3.18}$$

In order to prevent abrupt changes in the microgrid power profile at the point of common coupling to the utility grid, the following linear constraint should be imposed.

$$\begin{aligned}-u_{g_k} \leq & p_{bat_k}^{gc} + p_{bat_k}^{rc} - p_{bat_k}^{gd} - p_{bat_k}^{rd} + p_{d_k} \\ & - p_{bat_{k-1}}^{gc} - p_{bat_{k-1}}^{rc} + p_{bat_{k-1}}^{gd} + p_{bat_{k-1}}^{rd} \leq u_{g_k} \\ & \forall k \in [1, N_h],\end{aligned} \tag{3.19}$$

where u_g is an auxiliary optimization variable representing the magnitude of the variations in grid power rates in consecutive horizon time-steps.

The following constraint in conjunction with a term in the cost reduces the difference between the microgrid minimum and maximum powers at the point of coupling to the grid

$$p_g^{min}1 \leq p_{bat}^{gc} + p_{bat}^{rc} - p_{bat}^{gd} - p_{bat}^{rd} + p_d \leq p_g^{max}1, \tag{3.20}$$

where p_g^{min} and p_g^{max} are scalar optimization variables corresponding to minimum and maximum grid power rates.

The following inequality in (3.21) is also added to reduce the peak usage over some baseline denoted by p_g^{base}

$$p_{bat}^{gc} + p_{bat}^{rc} - p_{bat}^{gd} - p_{bat}^{rd} + p_d \leq p_g^{base}1 + p_g^{ob}1. \tag{3.21}$$

The optimization problem being solved at each step of the rolling horizon controller is as follows

$$
\begin{aligned}
\min \quad & (c_{batg}^T p_{bat}^{gc} + c_{batg}^T p_{bat}^{gd} + c_{batr}^T p_{bat}^{rc} + c_{batr}^T p_{bat}^{rd} \\
& + c_{smg}^T u_g + c_{smb}^T u_b \\
& + c_{peak} p_g^{ob} + c_{flat}(p_g^{max} - p_g^{min}) \\
& + (c_{buy}^T - c_{sell}^T) p_b + c_{sell}^T (p_d + p_{bat}^{gc} + p_{bat}^{rc} - p_{bat}^{gd} - p_{bat}^{rd})) \\
\text{subject to:} & \\
& p_b \geq p_d + p_{bat}^{gc} + p_{bat}^{rc} - p_{bat}^{gd} - p_{bat}^{rd}, \\
& p_b \geq 0 \\
& + \text{the linear constraints in (3.9)-(3.21).}
\end{aligned}
\tag{3.22}
$$

Since the optimization problem in (3.22) is linear and contains both continuous and binary decision variables, at each time-step a MILP problem is solved and the optimal values for the following decision variables are obtained.

$$
\begin{aligned}
& p_{bat}^{gc}, p_{bat}^{rc}, p_{bat}^{gd}, p_{bat}^{rd}, p_b \in \mathbb{R}^{N_h} \\
& u_b, u_g \in \mathbb{R}^{N_h} \\
& p_g^{ob}, p_g^{max}, p_g^{min} \in \mathbb{R} \\
& \delta_{cd}, \delta_r \in \mathbb{Z}^{N_h}.
\end{aligned}
\tag{3.23}
$$

The non-robust formulation presented in this section is based on the assumption that electricity demand and price signals are precisely predicted. However, there can be considerable uncertainty in predicted values of demand and prices, and the solution obtained through optimization must be robust with respect to the prediction errors. If unaccounted, these uncertainties may degrade the system performance and lead to sub-optimal solutions to the energy management problem. The goal here is to design a robust controller which accounts for these uncertainties in the system. The rest of this chapter is concerned with developing a CVaR-based controller which models the uncertainties in electricity demand and prices with a Gaussian distribution around their predicted nominal values.

3.2 A Brief Introduction on CVaR

Let $f(x, y)$ be the loss associated with a set of decision variables denoted by x and random model parameters y. The objective is to obtain the optimal value of the decision variable x which would minimize the loss subject to uncertainty in parameter y. A conservative solution to this problem is to find the set of decision variables that would minimize the worst-case cost for all possible realizations of y, i.e.,

$$\min_{x} \quad \max_{y} \quad f(x, y) \tag{3.24}$$

Alternative methods using a probabilistic framework where the probability density function of y denoted by $\mathcal{P}_y$ is known may yield less conservative solutions to this problem. One possible solution can be obtained by minimizing the β-percentile of the distribution associated with $f(x, y)$ induced by $\mathcal{P}_y$, β-VaR, defined as

$$\beta\text{-}VaR \triangleq min\{\alpha \in \mathbb{R} : \ P\{f(x, y) \leq \alpha\} \geq \beta\} \text{ for } 0 \leq \beta \leq 1. \tag{3.25}$$

In other words, for a given confidence level β, β-VaR is defined as the smallest cost α, such that, probability of losses above that level is at most $1-\beta$. This has been a very popular risk measure in finance and portfolio optimization, e.g. see Fabozzi et al. [2007]. However, VaR suffers from undesirable mathematical properties like lack of convexity and subadditivity which makes it unattractive in practical optimization problems(Artzner et al. [1999]). To avoid these problems, an alternative risk measure, CVaR for a given confidence level β, is defined as

$$\beta\text{-}CVaR \triangleq \mathbb{E}_y(f(x,y)|f(x,y) \geqslant \beta\text{-}VaR) \tag{3.26}$$

which is the conditional expected value of the cost, conditioned on its value exceeding the β-percentile.

In contrast to conventional robust optimization approaches, minimization of CVaR offers more flexibility in selection of the objective and can potentially improve performance by using distributional information on the uncertain parameter y. In fact, minimizing CVaR of the cost, minimizes the risk of the system being exposed to high losses rather than minimizing the worst-case cost. Moreover, for linear cost functions, minimizing CVaR can be formulated as a simple linear programming problem which makes it attractive in practical applications.

Similarly, for a given confidence level β, β-$CVaR$ is the conditional expectation of costs exceeding β-VaR,

$$\beta\text{-}CVaR \triangleq \mathbb{E}_y(f(x,y)|f(x,y) \geqslant \beta\text{-}VaR), \tag{3.27}$$

where $\mathbb{E}_y$ is the expectation of $f(x,y)$ for a fixed x over y.

Figure 3.1 illustrates the definition of VaR and CVaR with confidence level β.

The CVaR in (3.27) can be approximated to take a linear form as demonstrated in (Rockafellar and Uryasev [2000]). To this end, note that the conditional expectation

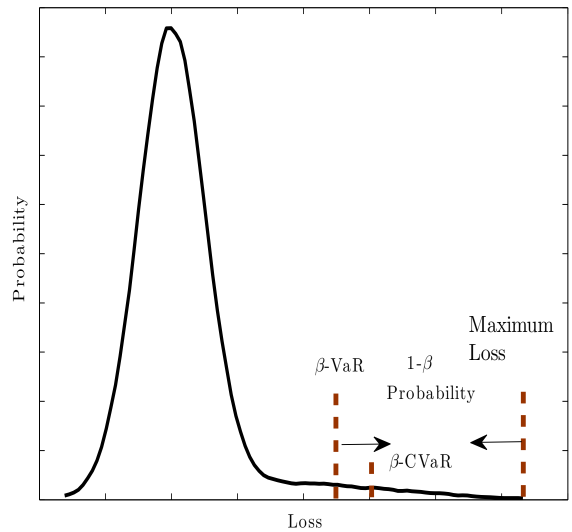

Figure 3.1: Graphical Representation of β-VaR and β-$CVaR$

in (3.27) can be rewritten as

$$\beta\text{-}CVaR = \frac{1}{P(f \geqslant \beta\text{-}VaR)} \int_{f(x,y)\geqslant\alpha} f(x,y)p(y)dy. \tag{3.28}$$

Note that $P(f \geqslant \beta\text{-}VaR)$ is equal to $1-\beta$. Thus, we have

$$\beta\text{-}CVaR = \frac{1}{1-\beta} \int_{f(x,y)\geqslant\alpha} f(x,y)p(y)dy, \tag{3.29}$$

Let us define F_β on $X \to \mathbb{R}$ in terms of β-$CVaR$ and β-VaR defined in (3.29) and (3.25), respectively.

$$\begin{aligned} F_\beta(x,\alpha) &= \alpha + \frac{1}{1-\beta} \int_{f(x,y)\geq\alpha} (f(x,y)-\alpha)p(y)dy \\ &= \alpha + \frac{1}{1-\beta} \int \left[f(x,y)-\alpha\right]^+ p(y)dy, \end{aligned} \tag{3.30}$$

where

$$\beta\text{-}CVaR = min_{\alpha \in \mathbb{R}} F_\beta(x,\alpha), \tag{3.31}$$

and

$$[t]^+ = \begin{cases} t & t > 0 \\ \\ 0 & \text{otherwise.} \end{cases} \tag{3.32}$$

The integral in (3.30) can be approximated by generating samples of y drawn from p_y, i.e.,

$$F_\beta(x,\alpha) \approx \alpha + \frac{1}{N(1-\beta)} \sum_{i=1}^{N} \left[f(x,y_i) - \alpha\right]^+, \tag{3.33}$$

where α is the $\beta\text{-}VaR$, N is the number of samples generated to approximate the cost distribution, and y_i refers to the i^{th} generated sample of the uncertain parameters vector.

The auxiliary variables $z_i|_{i=1}^{N}$ are defined to replace $[.]^+$ as follows

$$F_\beta(x,\alpha) \approx \alpha + \frac{1}{N(1-\beta)} \sum_{i=1}^{N} z_i, \tag{3.34}$$

where

$$z_i \triangleq [(f(x,y_i) - \alpha]^+ = max(0, f(x,y_i) - \alpha). \tag{3.35}$$

Finally, the equivalent optimization problem for minimizing $\beta\text{-}CVaR$ is formulated as

$$\begin{aligned} \min_{\alpha,x,z_i} \quad & \left(\alpha + \frac{1}{N(1-\beta)} \sum_{i=1}^{N} z_i\right) \\ \text{subject to:} \quad & z_i \geqslant 0, \\ & z_i \geqslant f(x,y_i) - \alpha. \end{aligned} \tag{3.36}$$

3.3 CVaR Optimization-based Rolling Horizon Energy Management

This section assumes that the electricity demand and prices are subject to uncertainty and an online optimal rolling horizon-based controller is presented to account for the fluctuations of these signals. The proposed method employs scenario-based minimization of CVaR of the cost, considering joint Gaussian uncertainty in the electricity demand and prices around their nominal predicted values. The resulting optimization problem in each step of the rolling horizon is of a MILP form.

The control values are optimized considering the following cost function associated with the decisions and system parameters,

$$\begin{aligned} J \triangleq & c_{batg}^T p_{bat}^{gc} + c_{batg}^T p_{bat}^{gd} + c_{batr}^T p_{bat}^{rc} + c_{batr}^T p_{bat}^{rd} \quad (a) \\ & + c_{smg}^T u_g + c_{smb}^T u_b \quad (b) \\ & + c_{peak} p_g^{ob} + c_{flat}(p_g^{max} - p_g^{min}) \quad (c) \\ & + C_u \quad (d). \end{aligned} \tag{3.37}$$

The battery operating costs, battery and grid signal smoothing costs, and grid signal flattening cost remain similar to those in the previous section. The last term in (d), which is uncertain here, represents the actual cost of electricity bought/sold from/to the utility grid and is defined as

$$C_u = c_{buy}^T p_b + c_{sell}^T p_s, \tag{3.38}$$

where c_{buy} and c_{sell} represent the electricity buying and selling prices, and p_b and p_s are time-averaged energy bought or sold, respectively. Here, unlike the non-robust formulation, both electricity prices and net demand could be subject to uncertainty. Consequently, this makes time-averaged buy/sell energies as a function of demand, uncertain as well.

Incorporating the aforementioned loss function in (3.37), into the CVaR optimization yields the following optimization problem

$$
\begin{aligned}
\min_{\alpha,x,z_i} \quad & \left(\alpha + \frac{1}{N(1-\beta)}\sum_{i=1}^{N} z_i\right) \\
\text{subject to:} \quad & \\
& c_{batg}^T p_{bat}^{gc} + c_{batg}^T p_{bat}^{gd} + c_{batr}^T p_{bat}^{rc} + c_{batr}^T p_{bat}^{rd} \\
& + c_{smg}^T u_g^i + c_{smb}^T u_b \\
& + c_{peak} p_g^{ob^i} + c_{flat}(p_g^{max^i} - p_g^{min^i}) \\
& + c_{buy,i}^T p_b^i + c_{sell,i}^T (p_d^i + p_{bat}^{gc} + p_{bat}^{rc} - p_{bat}^{gd} - p_{bat}^{rd} - p_b^i) \leq z_i + \alpha, \\
& z_i \geq 0, \\
& p_b^i \geq p_d^i + p_{bat}^{gc} + p_{bat}^{rc} - p_{bat}^{gd} - p_{bat}^{rd} \quad (a), \\
& p_b^i \geq 0 \quad (b), \\
& \forall i \in \{1, \ldots, N\},
\end{aligned}
\tag{3.39}
$$

where variables with index i correspond to the i^{th} generated sample vector which is drawn from a certain measure $\mathcal{P}_y$. Here, the uncertain vector consists of the electricity prices and net demand signal. It is worthy to note that constraints (3.39) (a) and (b) are imposed by removing the max function used in definition of time-averaged energy bought from the grid as follows

$$p_b^i \triangleq \max\left(p_d^i + p_{bat}^{gc} + p_{bat}^{rc} - p_{bat}^{gd} - p_{bat}^{rd}, 0\right). \tag{3.40}$$

3.3.1 Additional Constraints

The battery energy, power rate, battery signal smoothness , and red zone constraints in (3.9)-(3.18) remain unchanged. The grid signal smoothing, peak shaving, and flattening constraints are replaced with the following forms

$$\begin{aligned} -u_{g_k}^i \leq & p_{bat_k}^{gc} + p_{bat_k}^{rc} - p_{bat_k}^{gd} - p_{bat_k}^{rd} + p_{d_k}^i \\ & - p_{bat_{k-1}}^{gc} - p_{bat_{k-1}}^{rc} + p_{bat_{k-1}}^{gd} + p_{bat_{k-1}}^{rd} - p_{d_{k-1}}^i \leq u_{g_k}^i \\ & \forall i = 1, ..., N, k \in [1, N_h], \end{aligned} \tag{3.41}$$

here u_g^i is an auxiliary variable corresponding to the i^{th} generated sample vector of net demand.

$$p_g^{min,i}1 \leq p_{bat}^{gc} + p_{bat}^{rc} - p_{bat}^{gd} - p_{bat}^{rd} + p_d^i \leq p_g^{max,i} \quad \forall i = 1, ..., N, \tag{3.42}$$

where $p_g^{min^i}$ and $p_g^{max^i}$ are the auxiliary optimization variables indicating the maximum and minimum grid power rates corresponding to i^{th} sample of the net demand.

$$p_{bat}^{gc} + p_{bat}^{rc} - p_{bat}^{gd} - p_{bat}^{rd} + p_d^i \leq p_g^{base}1 + p_g^{ob,i}1 \quad \forall i = 1, ..., N, \tag{3.43}$$

Since the optimization problem in (3.39) is linear and contains both continuous and binary decision variables, at each time-step a MILP problem is solved to find the optimal values for the following decision variables

$$
\begin{aligned}
& p_{bat}^{gc}, p_{bat}^{rc}, p_{bat}^{gd}, p_{bat}^{rd} \in \mathbb{R}^{N_h} \\
& u_b, u_g^i, p_{buy}^i \in \mathbb{R}^{N_h} \quad \text{for} \quad i = 1, ..., N \\
& p_g^{ob,i}, p_g^{max,i}, p_g^{min,i}, z^i \in \mathbb{R} \quad \text{for} \quad i = 1, ..., N \\
& \alpha \in \mathbb{R} \\
& \delta_{cd}, \delta_r \in \mathbb{Z}^{N_h}
\end{aligned} \tag{3.44}
$$

subject to extra linear constraints (3.9)-(3.18),(3.41)-(3.43).

The battery charge/discharge command is simply computed from the first sample of the optimal decision vectors as

Table 3.1: Decisions on Battery Activity

δ_{cd}	δ_r	Charging Power	Discharging Power
0	0	0	$p_{bat}^{gd}(1)$
0	1	0	$p_{bat}^{rd}(1)$
1	0	$p_{bat}^{gc}(1)$	0
1	1	$p_{bat}^{rc}(1)$	0

3.4 Simulation Results

Simulations are performed on a commercial/residential setting data (with peak usage less than 24 kW) provided by Burlington Hydro Inc, with winter time of use electricity pricing, i.e., 6.2 ¢/kWh 7pm-7am, 9.2 ¢/kWh 11am-5pm, 10.8 ¢/kWh 7am-11am and 5pm-7pm and cost of selling energy back to the grid, i.e., 5 ¢/kWh 7am-7pm (Independent electricy system operator, IESO). All other costs including the flattening cost, grid and battery signal smoothing costs are set to small non-zero values. The battery characteristics are $E_{bat}^{min} = 0kWh$, $E_{bat}^{max} = 50kWh$,

$p_{bat}^{gc,max} = p_{bat}^{gd,max} = p_{bat}^{rc,max} = p_{bat}^{rd,max} = 10kW$, $T^{maxon} = T^{minoff} = 2h$, $P_{bat}^{loss} = 0$, $\eta_c = 0.95$, and $\eta_d = 0.9$. The time horizon used is 24 h with variable time-step vector h=[0.5 0.5 0.5 0.5 1 1 2 2 2 2 3 3 3 3], therefore $N_h = 14$ and the rolling horizon controller updates the decisions every half an hour. The hourly electricity buy/sell costs, i.e., c_{buy} and c_{sell} are determined by the time of day, hourly buy/sell prices, and employed rolling horizon vector h. For example at midnight c_{buy}=[3.1 3.1 3.1 3.1 6.2 6.2 12.4 17 21.6 20 27.6 29.2 23.2 18.6]^T and c_{sell}=[0 0 0 0 0 0 0 5 10 10 15 15 5 0]^T.

The energy management problem is formulated and solved in two different scenarios, the first one assumes that the only uncertain parameter is the net demand vector and the second one models the uncertainty in both electricity prices as well as net demand signal. The simulations are performed in one winter month under different magnitudes of actual uncertainty in the demand as well as electricity costs. Variations of the uncertain parameters are modeled by Gaussian distribution around their nominal values in the CVaR optimization. Standard deviation of the Gaussian noise in the optimization is set to Δp_d, $0.5\Delta c_{buy}$, and $0.5\Delta c_{sell}$, while actual uncertainties in the parameters are multiple of these constants. Here, Δp_d, Δc_{buy}, and Δc_{sell} are the square root of the nominal values of demand and electricity prices, respectively. Performance of the proposed robust approach is compared to its non-robust counterpart through a series of Monte-Carlo simulations in which the nominal data is perturbed by Gaussian noise with standard deviation of up to two times square root of the nominal values. Matlab is used with IBM ILOG CPLEX MILP as optimization solver using an Intel(R) Core(TM) i7-3770 CPU and 32 GB RAM to solve the optimization problem.

3.4.1 Impact of CVaR Factor β

A daily non-rolling horizon optimization is performed to investigate the effect of the values of β (0, 0.3, 0.6, 0.9) on the mean of cost distribution under presence of uncertainty in net demand. The average cost values are computed through a Monte-Carlo simulation with 1000 realized samples of demand which are generated from perturbing the nominal data by Gaussian noise with standard deviation of two times square root of the nominal values. From Table 3.2, it can be seen that different β values lead to slight difference in the daily average cost.

Table 3.2: Average daily cost with different values of β

β	0	0.3	0.6	0.9
Cost($)	15.79	15.82	15.84	15.8642

In the rest of this thesis, all the CVaR simulations are based on $\beta = 0.9$. Figure 3.2 depicts the expected shortfall (10%) of monthly cost distribution for non-robust and robust rolling horizon controllers in a fixed uncertainty level of demand, i.e., $2\Delta p_d$. A Monte-Carlo simulation with 1000 samples is performed to obtain the cost distribution in the specified uncertainty level. This provides a better insight of the CVaR objective which is to minimize the expected losses exceeding a certain range.

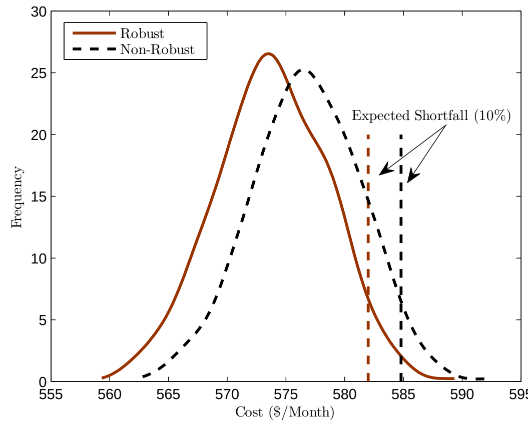

Figure 3.2: Comparison of expected shortfall (10%) of cost distribution for the non-robust and robust controllers in a fixed uncertainty level of net demand, i.e., $2\Delta p_d$.

3.4.2 Comparing Performance of Robust Controller to its Non-robust Counterpart under Presence of Uncertainty in Net Demand

In the first scenario the net electricity demand is the only uncertain parameter and the number of generated samples in the optimization is set to $N = 100$. The proposed approach models the uncertainty based on a Gaussian Distribution with standard deviation of Δp_d. Here Δp_d is defined as the square root of the nominal values. The monthly saving results are plotted in Figures 3.3 and 3.4 with two different maximum battery energy level. It is worthy to note that the net saving of the non-robust controller exceeds that of its robust counterpart at small levels of uncertainty in the demand. This is the price that the robust controller has to pay for better performance at higher uncertainty levels. Moreover, with smaller battery capacities ($E_{bat}^{max} = 50$), the gap between savings of the robust and non-robust controller is noticeably higher than in the case with larger battery capacity ($E_{bat}^{max} = 100$). This is due to the fact that there is no penalty in battery usage and non-robust controller exploits the batteries to compensate for the non-optimal decisions.

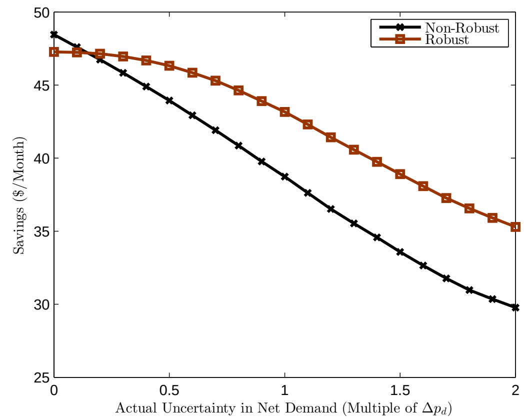

Figure 3.3: Comparison of the non-robust and robust controllers under uncertainty of net demand with $E_{bat}^{max} = 50$, winter time of use electricity pricing, i.e., 6.2 ¢/kWh 7pm-7am, 9.2 ¢/kWh 11am-5pm, 10.8 ¢/kWh 7am-11am and 5pm-7pm and cost of selling energy back to the grid, i.e., 5 ¢/kWh 7am-7pm. Standard deviation of the Gaussian distribution in the robust controller is set to Δp_d.

3.4.3 Comparing Performance of Robust Controller to its Non-robust Counterpart under Presence of Uncertainty in Net Demand and Electricity Prices

As stated before, the second scenario assumes that electricity prices are exposed to uncertainty too. Therefore, the vector of uncertain parameters consists of both electricity prices and demand, and hence a sufficiently large number of samples should be generated to obtain a precise approximation of the cost distribution. Table 3.3 shows the impact of number of samples on the optimization computational time per time-step of the rolling horizon controller as well as cost improvement comparing to

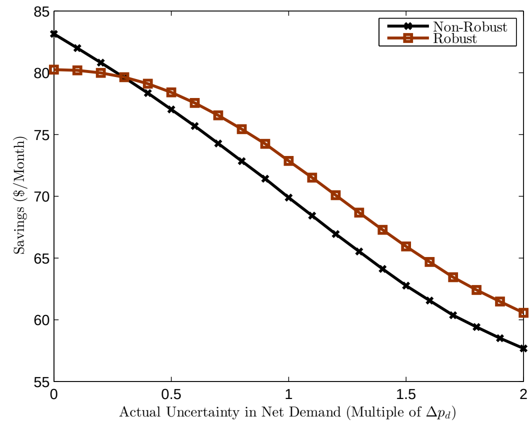

Figure 3.4: Comparison of the non-robust and robust controllers under uncertainty of net demand with $E_{bat}^{max} = 100$, winter time of use electricity pricing, i.e., 6.2 ¢/kWh 7pm-7am, 9.2 ¢/kWh 11am-5pm, 10.8 ¢/kWh 7am-11am and 5pm-7pm and cost of selling energy back to the grid, i.e., 5 ¢/kWh 7am-7pm. Standard deviation of the Gaussian distribution in the robust controller is set to Δp_d.

the non-robust controller.

A similar CVaR-based approach with $N = 300$ is used to model the joint uncertainty in electricity prices and demand vector. It should be noted that standard deviation of the Gaussian distribution used in the optimization is set to Δp_d in net demand signal, $0.5\Delta c_{buy}$ and $0.5\Delta c_{sell}$ in the electricity prices. Here, $\Delta p_d, \Delta c_{buy}, \Delta c_{sell}$ are defined as the square root of the nominal values. The monthly savings are plotted as a function of different magnitudes of actual uncertainty in demand in Figure 3.5 and actual uncertainty in costs in Figure 3.6. Figure 3.5 presents the monthly saving of the controllers at three different levels of uncertainty in cost of buying electricity, i.e., $0.5\Delta c_{buy}$, Δc_{buy}, and $1.5\Delta c_{buy}$ in (a), (b), and (c), respectively. The uncertainty levels are controlled by standard deviation of the Gaussian noise generated to evaluate performance of the controllers. It is worth noting that net saving of the non-robust

Table 3.3: Impact of the number of samples generated to approximate the cost distribution, i.e., N on the computational time per time-step of the rolling horizon controller (using an Intel(R) Core(TM) i7-3770 CPU and 32 GB RAM) and cost improvement over the non-robust controller

Approach and Number of Samples	Optimization Time(s)	Cost Improvement
CVaR with N=100	5	4.7%
CVaR with N=200	10	17.75%
CVaR with N=300	12	21%

controller exceeds that of its robust counterpart at small degrees of uncertainty in demand signal. This is the price that robust controller has to pay for better performance at higher uncertainty values. Moreover, the smallest uncertainty level in demand for which the robust controller outperforms its non-robust counterpart decreases from Figure 3.5 (a) to (c). Figure 3.6 also presents the monthly saving of the controllers at three different levels of uncertainty in net demand, i.e., $0.5\Delta p_d$, Δp_d, and $1.5\Delta p_d$ in (a), (b), and (c), respectively. It is pointed out that as the uncertainty in demand increases from Figure 3.6 (a) to (c), the gap in the savings of the controllers increases as well.

3.4.4 Grid and Battery Signals

This section presents the grid and battery power signals associated with the proposed robust controller under joint uncertainty of demand and electricity prices. The simulations are performed using the same commercial/residential setting as that in the previous section but with different battery specifications, i.e., $E_{bat}^{min} = 0kWh$, $E_{bat}^{max} =$

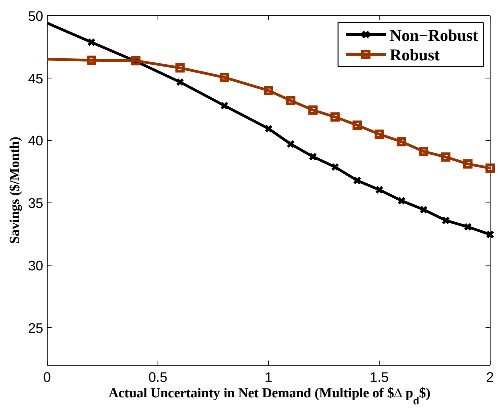

(a)

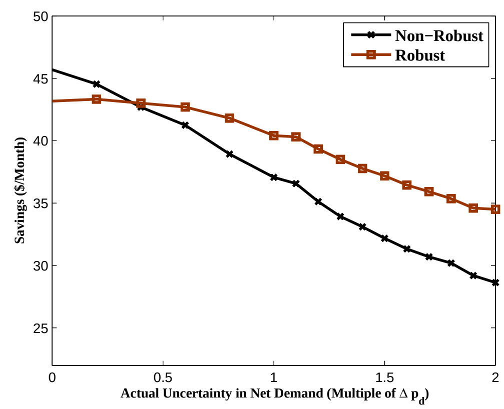

(b)

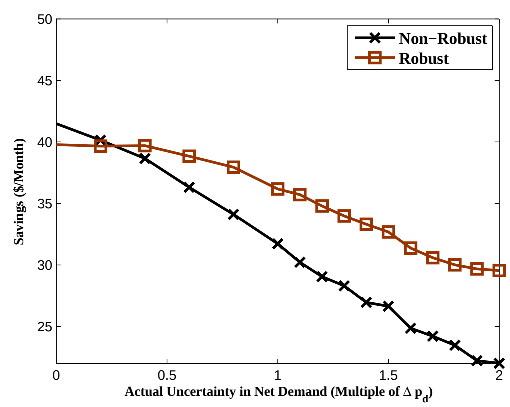

(c)

Figure 3.5: Comparison of the robust controller to its non-robust counterpart in the presence of uncertainty in both electricity prices and demand signal. Performance is plotted as a function of actual uncertainty in demand as a multiple of Δp_d along the horizontal axis. The uncertainty level in c_{buy} is set to $0.5\Delta c_{buy}$, Δc_{buy}, and $1.5\Delta c_{buy}$ in (a), (b), and (c), respectively.

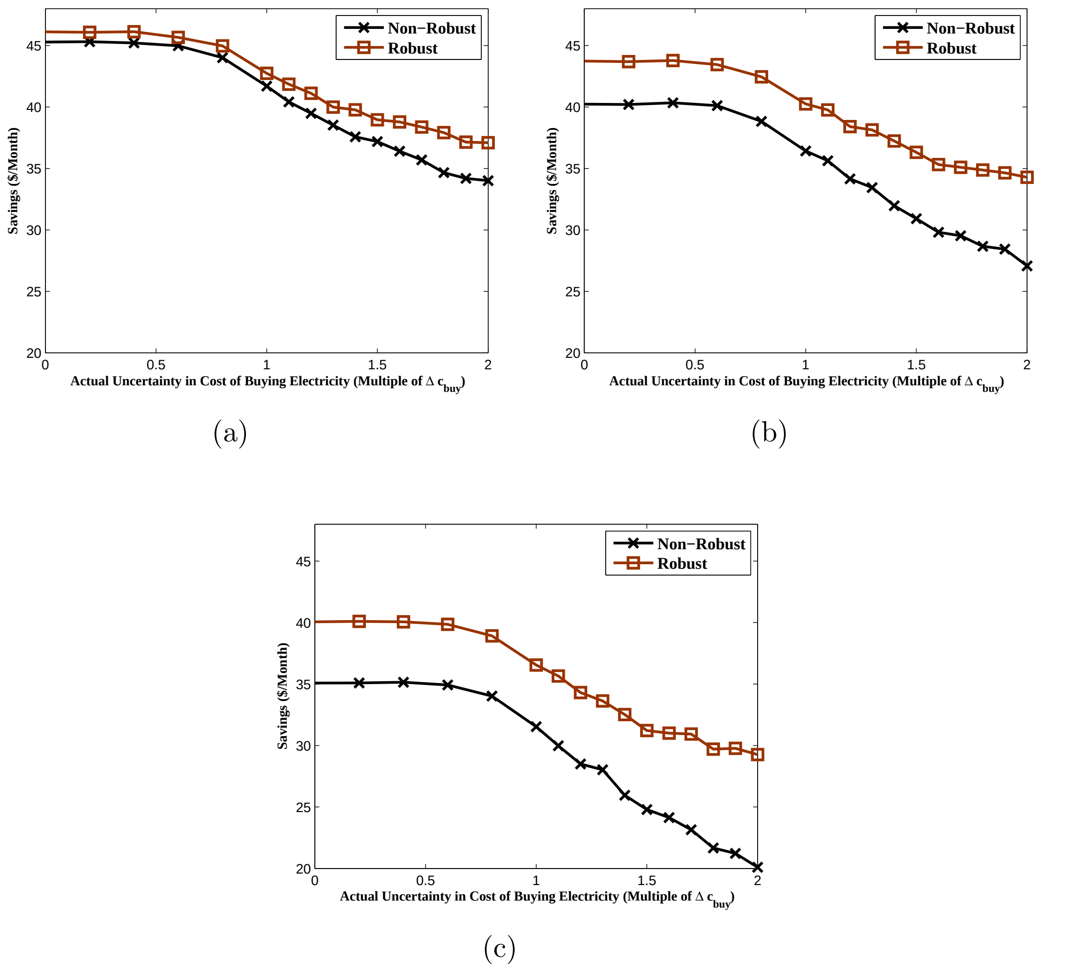

Figure 3.6: Comparison of the robust controller to its non-robust counterpart in the presence of uncertainty in both electricity prices and demand signal. Performance is plotted as a function of actual uncertainty in demand as a multiple of Δc_{buy} along the horizontal axis. The uncertainty level in p_d is set to $0.5\Delta p_d$, Δp_d, and $1.5\Delta p_d$ in (a),(b), and (c), respectively.

$15kWh$, $p_{bat}^{gc,max} = p_{bat}^{gd,max} = p_{bat}^{rc,max} = p_{bat}^{rd,max} = 3kW$, $T^{maxon} = 2h, T^{minoff} = 0.5h$, $P_{bat}^{loss} = 0$, $\eta_c = 0.95$,and $\eta_d = 0.9$. The horizon vector employed, as well as electricity buy/sell prices are similar to those in the previous section. Figure 3.7(a) depicts the grid power profile without the presence of controller. In Figure 3.7(b), the peak demand is penalized with $c_{peak} = 1$ \$/kW over a power baseline set to 9.5 kW and the controller attempts to keep the peak usage below that level. Figures 3.7(c) and (d) elucidate the flattening and smoothing of the grid signal with $c_{flat} = 0.1$ \$/kW and $c_{smg} = 0.1h$ \$/kW , respectively. A sub objective of battery usage with $c_{batg} = c_{batr} = 0.1h$ \$/kW is added and the effect is depicted in Figure 3.8(a). Then, battery smoothness is penalized with $c_{smb} = 0.05h$ \$/kW in Figure 3.8(b). Note that the red lines in grid power profiles indicate upper and lower envelopes of the grid power generated by $N = 1000$ different realizations of the demand signal within an uncertainty interval around the nominal values. It can be seen in Figures 3.8 (a) and (b) that penalizing batteries lead to less battery activity and consequently non-smoothness of the grid signal compared to the scenarios presented in Figures 3.7 (b),(c), and (d).

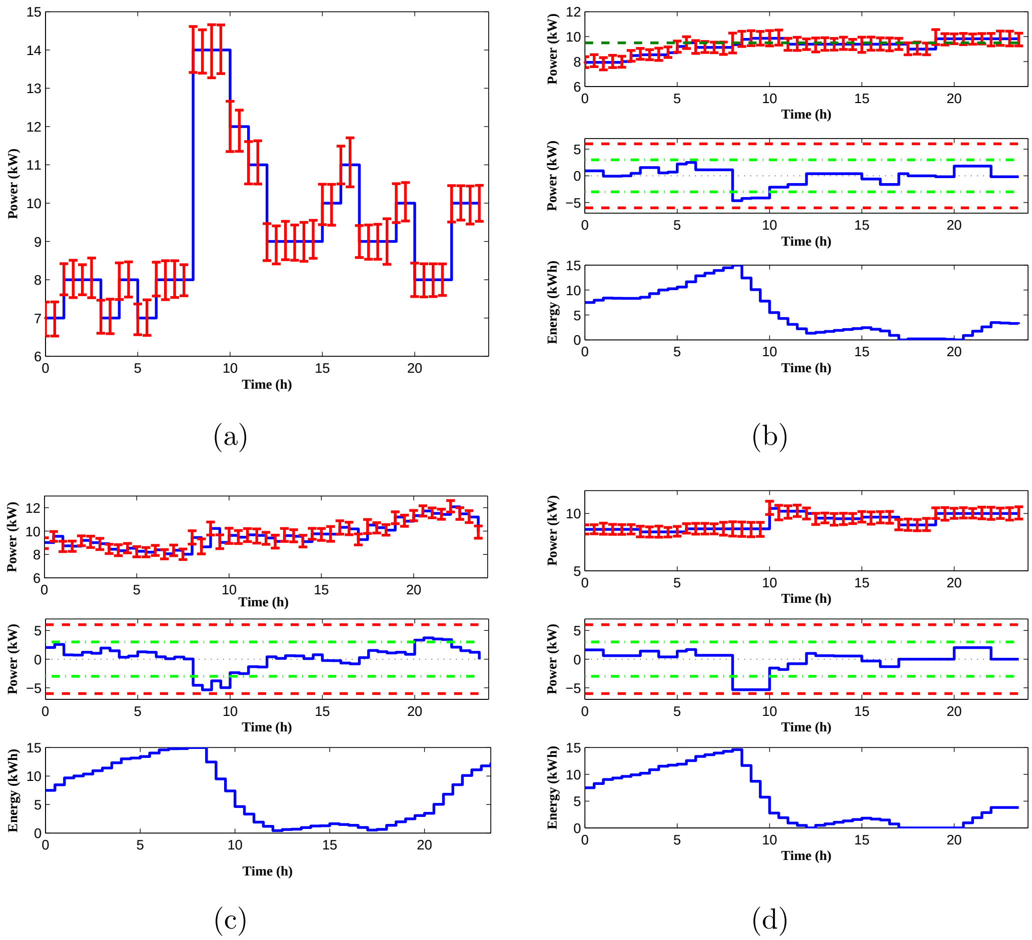

Figure 3.7: Grid and battery signals, (a) net demand profile; grid power profile with no controller, (b) grid power profile with only peak usage reduction (top figure); battery power profile (middle figure); battery energy profile (bottom figure) (c) grid power profile with only flattening objective (top figure); battery power profile (middle figure); battery energy profile (bottom figure) (d) grid power profile with only smoothing objective (top figure); battery power profile (middle figure); battery energy profile (bottom figure). Note the dot-dashed (green) line indicate green zone power rate limits, and the dashed red lines indicate maximum power rate limits in red zone.

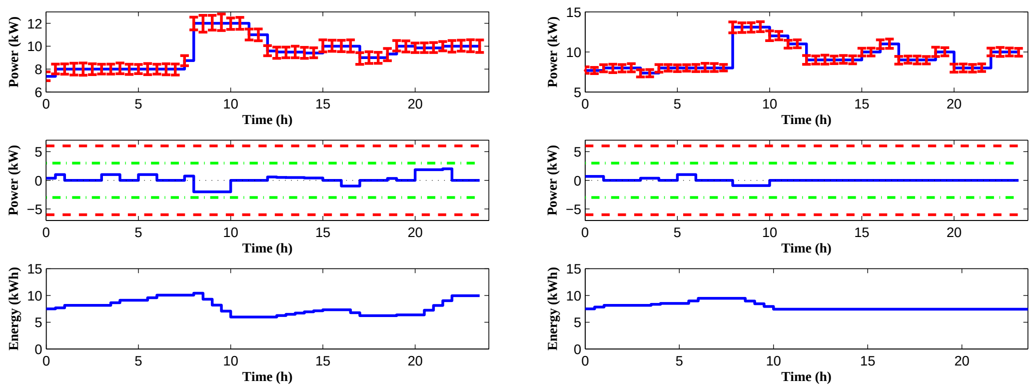

(a) (b)

Figure 3.8: Grid and battery signals, (a) grid power profile with grid flattening, smoothing, and battery usage penalty (top figure); battery power profile (middle figure); battery energy profile (bottom figure) (b) grid power profile with grid flattening, smoothing, battery usage, and battery smoothing sub objectives (top figure); battery power profile (middle figure); battery energy profile (bottom figure). Note the dot-dashed (green) line indicate green zone power rate limits, and the dashed red lines indicate maximum power rate limits in red zone.

Chapter 4

Energy Management based on Worst-case Conditional Value at Risk

4.1 Introduction

Imprecise assumption on the distribution of uncertain parameters can lead to poor performance of the stochastic approach introduced in the previous chapter. Moreover, the required number of sample scenarios to effectively approximate the CVaR minimization problem grows exponentially in proportion to the number of uncertain parameters. In order to speed up the optimization, a second method is proposed in which scenario-based minimization only takes samples from net demand with Gaussian uncertainty. Electricity prices are assumed to vary within known bounds and this uncertainty is handled by a worst-case robust approach. In particular, a reformulation of a constraint in CVaR minimization ensures that the worst-case cost with respect to price variations is considered in the optimization. In this chapter, the joint uncertainty problem is formulated and solved based on a combination of worst-case robust optimization and CVaR approach proposed in Chapter 3.

The rest of this chapter is organized as follows. In Section 4.2, a brief introduction on robust counterpart optimization for linear problems is presented. In Section 4.3, a worst-case CVaR-based approach is proposed to address the energy management problem under uncertainty of electricity prices as well as net demand. Finally, simulation results are presented in Section 4.4.

4.2 Robust Counterpart Formulation for Linear Optimization Problems

Consider the following Linear Problem (LP)

$$\begin{aligned} \min \quad & c^T x \\ s.t. \quad & \sum_j \tilde{a}_{ij} x_j \leq \tilde{b}_i \quad \forall i, \end{aligned} \tag{4.1}$$

where $\tilde{a}_{ij}$ and $\tilde{b}_i$ denote the actual values of the parameters under presence of uncertainty. Let us consider the i^{th} constraint where only the Left Hand Side (LHS) parameters are subject to uncertainty. The uncertainty can be modeled as following

$$\tilde{a}_{ij} = a_{ij} + \delta_{ij}\hat{a}_{ij} \quad \forall j \in J_i, \tag{4.2}$$

where a_{ij} and $\hat{a}_{ij}$ represent the nominal values and the positive perturbations of the uncertain parameters, respectively. δ_{ij} also denotes the random variables which are drawn from a known uncertainty set.

The main idea of robust counterpart optimization is to transform the above uncertain problem to a deterministic LP which attempts to find a feasible solution under all realizations of uncertain parameters within an uncertainty set. A comprehensive literature on different uncertainty sets and their corresponding robust counterpart can be found in Li et al. [2011]. In this thesis, a combined box and polyhedral uncertainty set is employed for formulating a robust counterpart optimization problem on a rolling horizon basis.

4.2.1 Box Uncertainty Set

A box uncertainty denoted by U with adjustable parameter L is defined as follows (Li et al. [2011])

$$U = \{\delta \mid |\delta_j| \leq L, \quad \forall j \in J_i\}, \tag{4.3}$$

where index j corresponds to the j^{th} uncertain coefficient in the i^{th} inequality. Figure 4.1 illustrates the shape of a box uncertainty set for (4.2) with $j = 1, 2$.

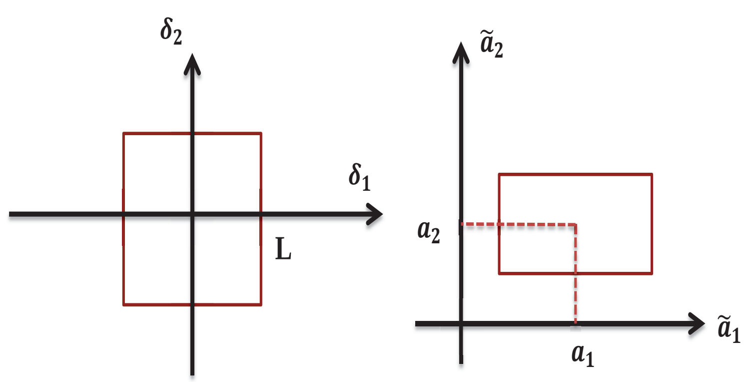

Figure 4.1: Illustration of box uncertainty set

4.2.2 Polyhedral Uncertainty Set

The polyhedral uncertainty set denoted by U_p is also described based on the ℓ-*norm* of the uncertain parameter as depicted in Figure 4.2.

$$U_p = \{\delta \mid \sum_j |\delta_j| \leq \Gamma\}, \tag{4.4}$$

where the size of the uncertainty set is determined by an adjustable parameter denoted by Γ.

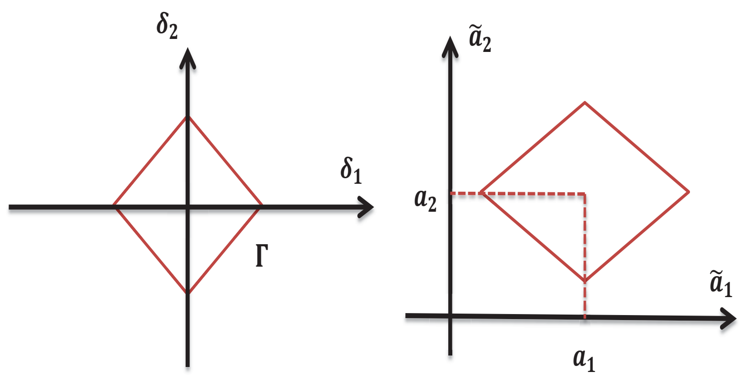

Figure 4.2: Illustration of polyhedral uncertainty set

4.2.3 "Box+Polyhedral" Uncertainty Set

This uncertainty set is defined as the intersection between the box and polyhedral uncertainty set as follows (Li et al. [2011])

$$U_{BP} = \{\delta \mid \sum_j |\delta_j| \leq \Gamma, \quad |\delta_j| \leq L, \quad \forall j \in J_i\}. \tag{4.5}$$

Figure 4.3 illustrates the combined box and polyhedral uncertainty set for different values of Γ. Please note that the intersection between these two uncertainty sets does not reduce to any of them if the following inequality constraint is satisfied

$$L \leq \Gamma \leq L|J_i| \tag{4.6}$$

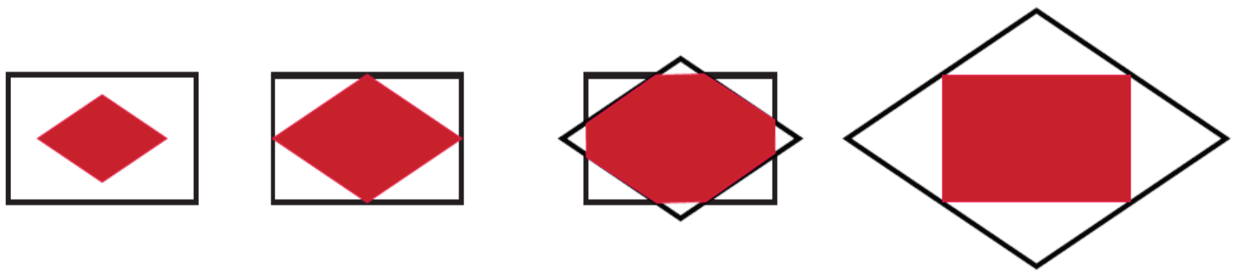

Figure 4.3: Illustration of combined box and polyhedral uncertainty set

The robust counterpart of the linear constraints in (4.1) induced by a "Box+Polyhedral" uncertainty set is as follows (see the proof in Li et al. [2011])

$$\begin{cases} \sum_j a_{ij}x_j + L\sum_j w_{ij} + \Gamma z_i \leq b_i \quad \text{(a)} \\ z_i + w_{ij} \geq \hat{a}_{ij}|x_j| \quad \forall j \in J_i \quad \text{(b)} \\ z_i, w_{ij} \geq 0, \end{cases} \tag{4.7}$$

where w_{ij} and z_i represent additional auxiliary optimization variables defined to obtain the robust counterpart LP. Note that the constraint (4.7) (b) contains absolute value function. In order to remove this non-linearity, an equivalent robust formulation can be obtained as follows

$$\begin{cases} \sum_j a_{ij}x_j + L\sum_j w_{ij} + \Gamma z_i \leq b_i \\ z_i + w_{ij} \geq \hat{a}_{ij}u_j, \quad \forall j \in J_i \\ -u_j \leq x_j \leq u_j, \quad \forall j \in J_i z_i, w_{ij} \geq 0, \end{cases} \tag{4.8}$$

where, the term x_j is substituted with auxiliary variable u_j and the constraints $-u_j \leq x_j \leq u_j$.

4.3 Application of a Worst-case CVaR Approach in Energy Management Problem under Uncertainty of Electricity Demand and Prices

In this section, a worst-case CVaR formulation of the energy management problem considering the worst-case cost with respect to price variations in a "Box+Polyhedral" uncertainty set is proposed. In other words, the constraints are ensured to remain feasible under all the realizations of electricity prices within the uncertainty set. Consider the following optimization problem

$$\begin{aligned} \min_{\alpha,x} \quad & \left(\alpha + \frac{1}{N(1-\beta)}\sum_{i=1}^{N} z_i\right) \\ \text{subject to:} \quad & z_i \geqslant 0, \\ & z_i \geqslant \tilde{f}(x, y_i, \tilde{c}) - \alpha, \end{aligned} \tag{4.9}$$

where $\tilde{f}(x, y_i, \tilde{c})$ represents the true value of the loss associated with a certain strategy x, true value of electricity prices denoted by $\tilde{c}$ and a set of demand samples denoted by y_i, generated from a Gaussian distribution and is defined as follows:

$$\begin{aligned}\tilde{f}(x, y_i, \tilde{c}) = {} & c_{batg}^T p_{bat}^{gc} + c_{batg}^T p_{bat}^{gd} + c_{batr}^T p_{bat}^{rc} + c_{batr}^T p_{bat}^{rd} \\ & + c_{smb}^T u_g^i + c_{smb}^T u_b \\ & + c_{peak} p_g^{ob^i} + c_{flat}(p_g^{max^i} - p_g^{min^i}) \\ & + (\tilde{c}_{buy}^T - \tilde{c}_{sell}^T) p_{buy}^i + \tilde{c}_{sell}^T (p_d^i + p_{bat}^{gc} + p_{bat}^{rc} - p_{bat}^{gd} - p_{bat}^{rd}) \\ & \text{for } i = 1, ..., N.\end{aligned} \tag{4.10}$$

In this chapter, the uncertainty in electricity prices are modeled with assumption of independent variations of buy/sell electricity price signals around their predicted nominal values and the uncertainty in these two parameters is modeled as follows

$$\tilde{c}_{buy} = c_{buy} + \delta_1 \hat{c}_{buy}, \tag{4.11}$$

$$\tilde{c}_{sell} = c_{sell} + \delta_2 \hat{c}_{sell}, \tag{4.12}$$

where c_{buy} and c_{sell} represent the nominal value of the parameters; $\hat{c}_{buy}$ and $\hat{c}_{sell}$ represent constant positive perturbation and δ_1 and δ_2 are random variables which are subject to uncertainty. Considering a "Box+Polyhedral" uncertainty set yields the following robust counterpart optimization problem

$$
\begin{aligned}
&\min_{\alpha,x,z_i} \quad \left(\alpha + \frac{1}{N(1-\beta)}\sum_{i=1}^{N} z_i\right) \\
&\text{subject to:} \\
&z_i \geqslant 0, \\
&z_i + \alpha \geqslant c_{batg}^T p_{bat}^{gc} + c_{batg}^T p_{bat}^{gd} + c_{batr}^T p_{bat}^{rc} + c_{batr}^T p_{bat}^{rd} \\
&+ c_{smb}^T u_g^i + c_{smb}^T u_b \\
&+ c_{peak} p_g^{ob^i} + c_{flat}(p_g^{max^i} - p_g^{min^i}) \\
&+ c_{buy}^T p_{buy}^i + c_{sell}^T(p_d^i + p_{bat}^{gc} + p_{bat}^{rc} - p_{bat}^{gd} - p_{bat}^{rd} - p_{buy}^i) \\
&+ \Psi^T w_1^i + \Psi^T w_2^i + \Gamma w_3^i \quad \text{for } i = 1, ..., N, \\
&w_{1j}^i + w_{3j}^i \geq \hat{c}_{buy}^T p_{buy}^i, \\
&w_{2j}^i + w_{3j}^i \geq \hat{c}_{sell}^T u^i, \\
&- u^i \leq (p_d^i + p_{bat}^{gc} + p_{bat}^{rc} - p_{bat}^{gd} - p_{bat}^{rd}) \leq u^i, \\
&\text{for} \quad j \in [1, N_h], i = 1, ..., N, \\
&+ \text{the linear constraints in (3.9)-(3.18), (3.41)-(3.43).}
\end{aligned}
\tag{4.13}
$$

Here, w_1,w_2, $u^i \in \mathbb{R}^{N_h}$ and $w_3 \in \mathbb{R}$ are additional auxiliary variables needed for the robust worst case optimization (Li et al. [2011]) and x refers to the optimization variables consisting of the following elements

$$
\begin{aligned}
&p_{bat}^{gc}, p_{bat}^{rc}, p_{bat}^{gd}, p_{bat}^{rd}, w_1, w_2 \in \mathbb{R}^{N_h} \\
&u_b, u_g^i, p_b^i \quad \in \mathbb{R}^{N_h} \quad (\text{for} i = 1, ..., N) \\
&p_g^{max,i}, p_g^{min,i}, z_i, \alpha, w_3 \in \mathbb{R} \quad (\text{for} \quad i = 1, ..., N) \\
&\delta_{cd}, \delta_r \in \mathbb{Z}^{N_h}.
\end{aligned}
\tag{4.14}
$$

Since the optimization problem in (4.13) is linear and contains both continuous and binary decision variables, at each time-step a MILP optimization problem is solved to find the optimal values of the variables in (4.14).

The battery charge/discharge command is simply computed from the first sample of the optimal decision vectors as shown in Table 4.1.

Table 4.1: Decisions on Battery Activity

δ_{cd}	δ_r	Charging Power	Discharging Power
0	0	0	$p_{bat}^{gd}(1)$
0	1	0	$p_{bat}^{rd}(1)$
1	0	$p_{bat}^{gc}(1)$	0
1	1	$p_{bat}^{rc}(1)$	0

4.4 Simulation Results

4.4.1 Comparing Performance of the Proposed Robust Controller to its Non-robust Counterpart under Presence of Uncertainty in Net Demand and Electricity Prices

Simulations are performed on a commercial/residential setting data (with peak usage less than 24 kW) provided by Burlington Hydro Inc, with winter time of use electricity pricing, i.e., 6.2 ¢/kWh 7pm-7am, 9.2 ¢/kWh 11am-5pm, 10.8 ¢/kWh 7am-11am and 5pm-7pm and selling price, i.e., 5 ¢/kWh 7am-7pm (Independent electricy system operator, IESO). All other costs including the flattening cost, grid and battery signal smoothing costs are set to small non-zero values. The battery characteristics are $E_{bat}^{min} = 0kWh$, $E_{bat}^{max} = 50kWh$, $p_{bat}^{gc,max} = p_{bat}^{gd,max} = p_{bat}^{rc,max} = p_{bat}^{rd,max} = 10kW$, $T^{maxon} = T^{minoff} = 2h$, $P_{bat}^{loss} = 0$, $\eta_c = 0.95$, and $\eta_d = 0.9$. The time horizon used is 24 h with variable time-step vector h=[0.5 0.5 0.5 0.5 1 1 2 2 2 2 3 3 3 3], therefore $N_h = 14$ and the rolling horizon controller updates the decisions every half an hour. The hourly electricity buy/sell costs, i.e., c_{buy} and c_{sell} are determined by the time of day, hourly buy/sell prices, and employed rolling horizon vector h. For example at midnight c_{buy}=[3.1 3.1 3.1 3.1 6.2 6.2 12.4 17 21.6 20 27.6 29.2 23.2 18.6]^T and c_{sell}=[0 0 0 0 0 0 0 5 10 10 15 15 5 0]^T. The assumptions on controller's robustness with respect to net demand signal (standard deviation of Gaussian noise used to model the demand variations) is preserved as in the previous chapter, i.e., Δp_d. The robust counterpart formulation of the problem is obtained with tuning the parameters of "Box+Polyhedral" uncertainty set, Ψ, and Γ to 1 and two times square root of N_h, respectively. The constant positive perturbations in modeling electricity prices, i.e., $\hat{c_{buy}}$ and $\hat{c_{sell}}$, are also set to square root of the nominal electricity buy and sell prices, respectively. The simulations are performed in one winter month under different magnitudes of actual uncertainty in the demand as well as electricity prices. Performance of the proposed robust approach is compared to its non-robust counterpart through a series of Monte-Carlo simulations in which the nominal data is perturbed by Gaussian noise with standard deviation of up to two times square root of the nominal values. Matlab is used with IBM ILOG CPLEX MILP as optimization solver using an Intel(R) Core(TM) i7-3770 CPU and 32 GB RAM to solve the optimization problem.

The monthly savings are plotted as a function of different magnitudes of actual uncertainty in demand in Figure 4.4 and actual uncertainty in costs in Figure 4.5. Figure 4.4 presents the monthly saving of the robust and non-robust controllers at three different levels of uncertainty in cost of buying electricity, i.e., $0.5\Delta c_{buy}$, Δc_{buy}, and $1.5\Delta c_{buy}$ in (a), (b), and (c), respectively. The uncertainty levels are controlled by standard deviation of the Gaussian noise generated to evaluate performance of the controllers. It is worth noting that net saving of the non-robust controller exceeds that of its robust counterpart at small degrees of uncertainty in demand signal. This is the price that the robust controller has to pay for better performance at higher uncertainty values. Moreover, the smallest uncertainty level in demand for which the robust controller outperforms its non-robust counterpart decreases from Figure 4.4 (a) to (c). Figure 4.5 also presents the monthly saving of the controllers at three different levels of uncertainty in net demand, i.e., $0.5\Delta p_d$, Δp_d, and $1.5\Delta p_d$ in (a), (b), and (c) , respectively. It is pointed out that as the uncertainty in demand increases from Figure 4.5 (a) to (c), the gap in the savings of the controllers increases as well.

4.4.2 Grid and Battery Signals

This section presents the grid and battery power signals associated with the proposed robust controller under joint uncertainty of demand and electricity prices. The simulations are performed using the same commercial/residential setting as that in the previous section but with different battery specifications, i.e., $E_{bat}^{min} = 0kWh$, $E_{bat}^{max} = 15kWh$, $p_{bat}^{gc,max} = p_{bat}^{gd,max} = p_{bat}^{rc,max} = p_{bat}^{rd,max} = 3kW$, $T^{maxon} = 2h, T^{minoff} = 0.5h$, $P_{bat}^{loss} = 0$, $\eta_c = 0.95$,and $\eta_d = 0.9$. The horizon vector employed, as well as electricity buy/sell prices are similar to those in the previous section. Figure 4.6(a) depicts the grid power profile without the presence of controller. In Figure 4.6(b), the peak

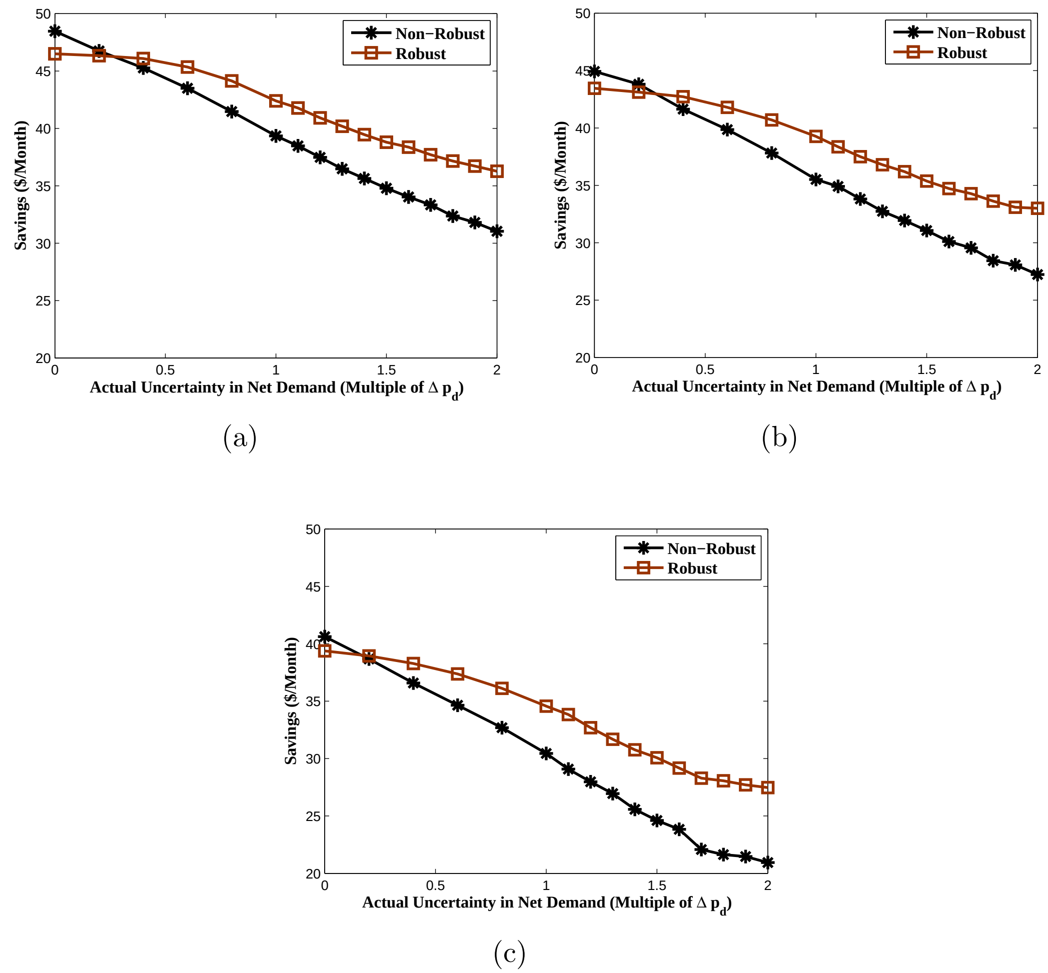

Figure 4.4: Comparison of the robust controller to its non-robust counterpart in the presence of uncertainty in both electricity prices and demand signal. Performance is plotted as a function of actual uncertainty in demand as a multiple of Δp_d along the horizontal axis. The uncertainty level in c_{buy} is set to $0.5\Delta c_{buy}$, Δc_{buy}, and $1.5\Delta c_{buy}$ in (a), (b), and (c), respectively.

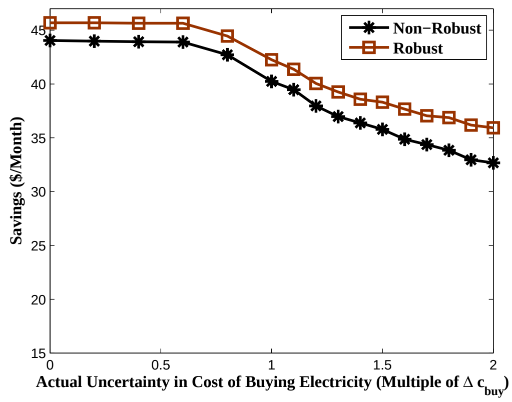

(a)

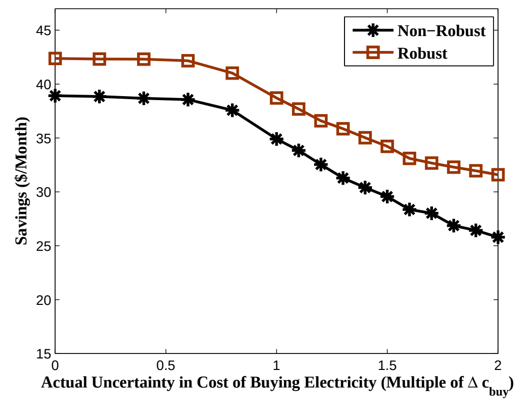

(b)

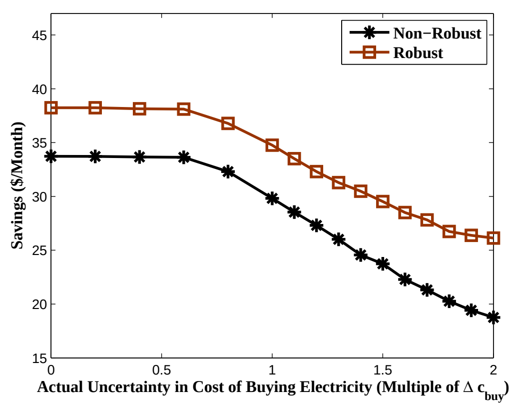

(c)

Figure 4.5: Comparison of the robust controller to its non-robust counterpart in the presence of uncertainty in both electricity prices and demand signal. Performance is plotted as a function of actual uncertainty in demand as a multiple of Δc_{buy} along the horizontal axis. The uncertainty level in p_d is set to $0.5\Delta p_d$, Δp_d, and $1.5\Delta p_d$ in (a),(b), and (c), respectively.

demand is penalized with $c_{peak} = 1$ \$/kW over a power baseline set to 9.5 kW and the controller attempts to keep the peak usage below that level. Figures 4.6(c) and (d) demonstrate the flattening and smoothing of the grid signal with $c_{flat} = 0.1$ \$/kW and $c_{smg} = 0.1h$ \$/kW, respectively. A sub objective of battery usage with $c_{batg} = c_{batr} = 0.1h$ \$/kW is added and the effect is depicted in Figure 4.7(e). Then, battery smoothness is penalized with $c_{smb} = 0.05h$ \$/kW in Figure 4.7(f). Note that the red lines in grid power profiles indicate upper and lower envelopes of the grid power generated by $N = 1000$ different realizations of the demand signal within an uncertainty interval around the nominal values. It can be seen in Figures 4.7 (a) and (b) that penalizing batteries lead to less battery activity and consequently non-smoothness of the grid signal compared to the scenarios presented in Figures 4.6 (b),(c), and (d).

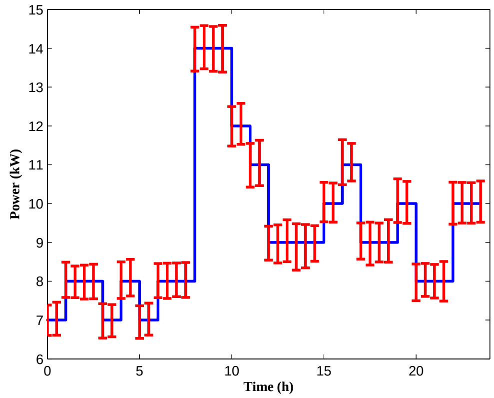

(a)

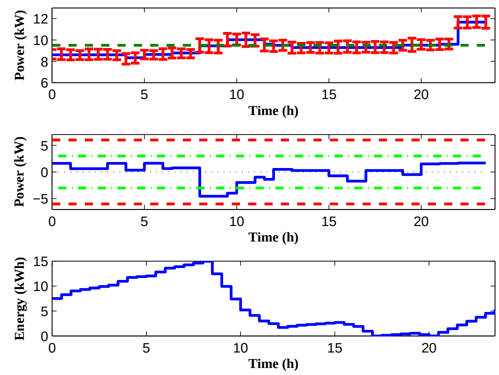

(b)

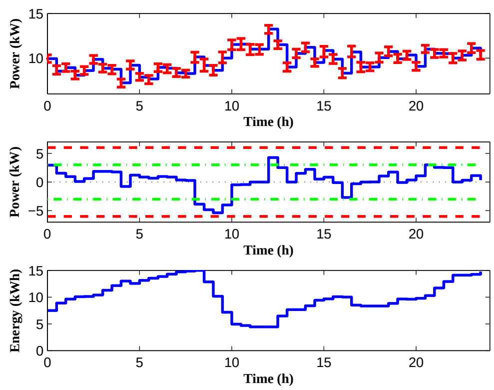

(c)

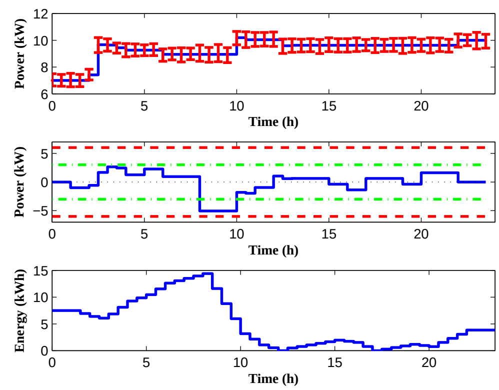

(d)

Figure 4.6: Grid and battery signals, (a) net demand profile; grid power profile with no controller, (b) grid power profile with only peak usage reduction (top figure); battery power profile (middle figure); battery energy profile (bottom figure), (c) grid power profile with only flattening objective (top figure); battery power profile (middle figure); battery energy profile (bottom figure), (d) grid power profile with only smoothing objective (top figure); battery power profile (middle figure); battery energy profile (bottom figure). Note the dot-dashed (green) line indicate green zone power rate limits, and the dashed red lines indicate maximum power rate limits in red zone.

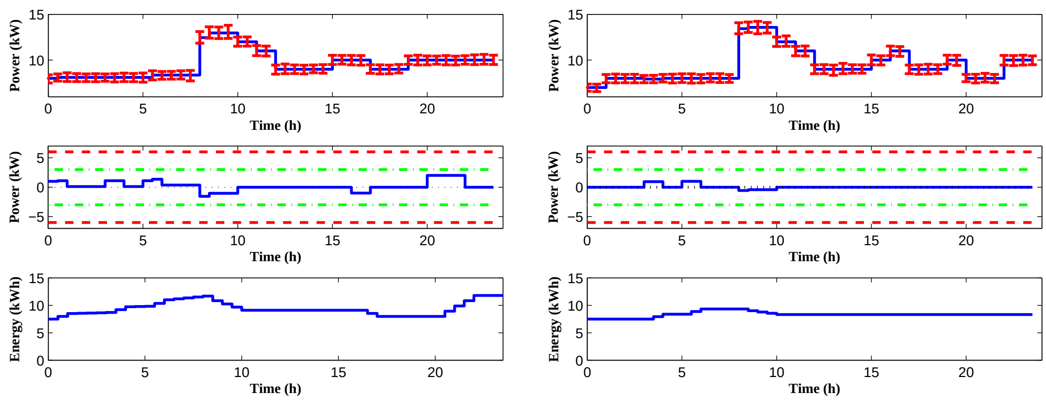

(a) (b)

Figure 4.7: Grid and battery signals, (a) grid power profile with grid flattening, smoothing, and battery usage penalty (top figure); battery power profile (middle figure); battery energy profile (bottom figure) (b) grid power profile with grid flattening, smoothing, battery usage, and battery smoothing sub objectives (top figure); battery power profile (middle figure); battery energy profile (bottom figure). Note the dot-dashed (green) line indicate green zone power rate limits, and the dashed red lines indicate maximum power rate limits in red zone.

Chapter 5

LP Formulations of Energy Management Optimization without Binary Variables

Growth in the number of integer variables may cause the MILP problems to become computationally intractable. This chapter aims at developing equivalent linear formulations of the proposed robust optimizations introduced in Chapters 3 and 4 without the binary variables, by simplifying the battery operation model. Furthermore, the performance of the resulting linear robust optimizations are evaluated and compared to their non-robust counterparts in different scenarios. The rest of this chapter is organized as follows. A linear formulation of the CVaR approach introduced in Chapter 3 is presented in Section 5.1. Section 5.2 introduces a linear formulation of the Worst-Case CVaR approach introduced in Chapter 4. This chapter is concluded by presenting simulation results in Section 5.3.

5.1 Linear CVaR

In this section, a rolling horizon controller is proposed to account for the uncertainties in net demand and electricity prices. The proposed controller employs a 24-hour ahead prediction window of net demand power vector and electricity prices to make optimal battery charge/discharge decisions at each time step.

The control values are optimized considering the following cost function associated with the decisions and system parameters,

$$\begin{aligned} J \triangleq & c_c p^+ - c_d p^- \quad (a) \\ & + c_{smg}^T u_g \quad (b) \\ & + c_{peak} p_g^{ob} + c_{flat}(p_g^{max} - p_g^{min}) \quad (c) \\ & + c_u \quad (d). \end{aligned} \tag{5.1}$$

The sum of the terms in (a) represents the cost associated with operating the batteries. Here, p^+ and p^- are power rates for charging and discharging the batteries and c_c and c_d are the associated costs. The term (b) penalizes the grid signal non-smoothness where, u_g represents the magnitude of the variations in battery and grid power rates in consecutive horizon time-steps and c_{smg} is the associated cost. The first term in (c) reduces the peak in demand at point of common coupling by penalizing excess demand p_g^{ob} over a baseline power rate p_g^{base} set by the user (see Malysz et al. [2014] for details). The second term flattens the grid power signal p_g by penalizing the difference between its maximum and minimum values. The last term in (d), which is uncertain, represents the actual cost of electricity bought/sold from/to the utility grid and is defined as follows

$$c_u \triangleq c_{buy}^T p_b + c_{sell}^T p_s, \tag{5.2}$$

where c_{buy} and c_{sell} represent the electricity buying and selling prices, and p_b and p_s are time-averaged energy bought or sold, respectively. They are defined as

$$p_b \triangleq \max\left(p_d + p_{bat}, 0\right), \tag{5.3}$$

$$\begin{aligned} p_s &\triangleq \min\left(p_d + p_{bat}, 0\right) \\ &= (p_d + p_{bat} - p_b), \end{aligned} \tag{5.4}$$

where p_{bat} represents total power of batteries and is related to individual charging/discharging powers as following

$$\begin{aligned} &p^+ = max(p_{bat}, 0), \\ &p_{bat} = p^+ + p^-. \end{aligned} \tag{5.5}$$

Substituting (5.4) in (5.2) yields

$$\begin{aligned} C_u = (c_{buy}^T - c_{sell}^T)p_b \\ + c_{sell}^T(p_d + p_{bat}). \end{aligned} \tag{5.6}$$

Assuming $c_{buy} \geq c_{sel}$ and $c_c > 0$, the nonlinearity introduced in the cost by the max function in (5.3) and (5.5) can be eliminated using the following constraints

$$
\begin{aligned}
&p_b \geq p_d + p_{bat}, \\
&p_b \geq 0, \\
&p^+ \geq p_{bat}, \\
&p^+ \geq 0.
\end{aligned}
\tag{5.7}
$$

Incorporating the loss function J in (5.1) into the CVaR optimization framework yields a Linear Programming (LP) problem as follows

$$
\min_{\alpha,x,z_i} \quad \left(\alpha + \frac{1}{N(1-\beta)} \sum_{i=1}^{N} z_i \right)
$$

subject to:

$$
\begin{aligned}
&c_c^T p^+ + c_d^T (p^+ - p_{bat}) \\
&+ c_{smg}^T u_g^i \\
&+ c_{peak} p_g^{ob,i} + c_{flat}(p_g^{max,i} - p_g^{min,i}) \\
&+ (c_{buy,i}^T - c_{sell,i}^T) p_b^i + c_{sell,i}^T (p_d^i + p_{bat}) \leq z_i + \alpha
\end{aligned}
\tag{5.8}
$$

$$
z_i \geq 0,
$$

$$
\begin{aligned}
&p_b^i \geq p_d^i + p_{bat} \\
&p_b^i \geq 0 \qquad \forall i \in \{1, \ldots, N\} \\
&p^+ \geq p_{bat}, \\
&p^+ \geq 0,
\end{aligned}
\tag{5.9}
$$

$$E_{bat}^{min} \leq \eta_c \sum_{i=1}^{k} h_i p^+ - p_{bat}^{loss} \sum_{i=1}^{k} h_i$$
$$-\eta_d^{-1} \sum_{i=1}^{k} h_i (p_{bat} - p^+) + E_{bat}^0 \leq E_{bat}^{max} \quad for \quad k \in [1, Nh], \tag{5.10}$$

$$0 \leq p_{bat} \leq p_{bat}^{max}$$
$$0 \leq p^+ \leq p^{max}, \tag{5.11}$$

$$\eta_c h^T p^+ - \eta_d^{-1} h^T (p_{bat} - p^+) - E_{bat}^{loss} h^T 1 =$$
$$E_{bat}^{final} - E_{bat}^0, \tag{5.12}$$

$$-\Delta p_{bat} h \leq p_{bat_k} - p_{bat_{k-1}} \leq \Delta p_{bat} h \quad , \tag{5.13}$$

$$-u_{g_k}^i \leq p_{bat_k} + p_{d_k}^i - p_{bat_{k-1}} - p_{d_{k-1}}^i \leq u_{g_k}^i$$
$$\forall i = 1, ..., N, k \in [1, N_h], \tag{5.14}$$

$$p_g^{min,i} 1 \leq p_{bat} + p_d^i \leq p_g^{max,i} \quad \forall i = 1, ..., N, \tag{5.15}$$

$$p_{bat} + p_d^i \leq p_g^{base} 1 + p_g^{ob,i} 1 \quad \forall i = 1, ..., N, \tag{5.16}$$

where variables with index i are additional optimization variables corresponding to the i^{th} generated sample vector which is drawn from a certain measure $\mathcal{P}_y$.

In this work, a discrete-time model for battery storage devices is employed as follows

$$E_{k+1} = E_k + \eta_c h_k {p^+}_k - \eta_d^{-1} h_k {p^-}_k - P_{bat}^{loss} h_k, \tag{5.17}$$

where E_k represents the energy of battery at time step k in kWh, h_k is the length of the time step measured in hours, P_{bat}^{loss} is the self discharging power of the battery in kW per hour, p^+ and p^-, η_c and η_d represent battery charging and discharging power and efficiency respectively. The inequality constraint in (5.10) ensures that the battery energy level remains within safe limits at each time step; here E_{bat}^0 is battery energy level at the beginning of the control horizon, and E_{bat}^{min} and E_{bat}^{max} denote minimum and maximum allowable battery energy levels. Battery powers are also constrained through (5.11), where the scalar constants p_{bat}^{max}, p^{max} represent the maximum battery rates.

The equality constraint (5.12) simply relates the battery initial energy level E_{bat}^0 to is final energy level E_{bat}^{final}, and is based on the battery model in (5.17). The inequality constraint in (5.13) imposes some smoothness on the battery activities. The microgrid power profile at the point of common coupling to the utility grid is smoothened via (5.14) and the associated term in the cost; here u_g^i is an auxiliary variable corresponding to the i^{th} generated sample vector of net demand. The constraint (5.15) in conjunction with a term in the cost reduces the difference between the microgrid minimum and maximum powers at the point of coupling to the grid. The inequality in (5.16) is also added to reduce the peak usage over some baseline denoted by p_g^{base}. The reader is referred to Malysz et al. [2014] for further information on the cost objective and constraints.

A Gaussian distribution is assumed to generate samples of net demand and electricity prices, but other distributions could easily be employed as well. At each time-step the LP problem defined in (5.8) is solved to find optimal values for the following decision variables

$$
\begin{aligned}
& p_{bat}, p^{+} \in \mathbb{R}^{N_h}, \\
& u_g^i, p_b^i \in \mathbb{R}^{N_h} \quad (\text{for} \quad i = 1, ..., N), \\
& p_g^{ob,i}, p_g^{max,i}, p_g^{min,i}, z_i, \alpha \in \mathbb{R} \quad (\text{for} \quad i = 1, ..., N).
\end{aligned} \tag{5.18}
$$

The battery charge/discharge command is simply computed from the first sample of the optimal decision vectors p^+ and $p_{bat} - p^+$.

5.2 Linear Worst-case CVaR

In this section, the joint uncertainty problem is formulated and solved based on a combination of Worst-case robust and CVaR approach. Particularly, variations of net demand is modeled by a Gaussian distribution while electricity prices are assumed to vary within an uncertainty set around their nominal values. A similar LP problem as the previous section is formulated and solved except that the constraints including electricity prices are "robustified" with respect to their worst case values. In other words, the constraints are ensured to remain feasible under all the realizations of electricity prices within the uncertainty set. The optimization problem to solve is given as

$$
\begin{aligned}
& \min_{\alpha, x, z_i} \quad \left(\alpha + \frac{1}{N(1-\beta)} \sum_{i=1}^{N} z_i \right) \\
& \text{subject to:} \quad z_i \geqslant 0 \\
& \qquad\qquad\quad z_i \geqslant \tilde{f}(x, y_i, \tilde{c}) - \alpha \\
& \qquad\qquad\quad + \text{the linear constraints in (5.9)-(5.16)},
\end{aligned} \tag{5.19}
$$

where $\tilde{f}(x, y_i, \tilde{c})$ represents true value of the loss associated with a certain strategy x, true value of electricity prices denoted by $\tilde{c}$ and a set of demand samples generated from a Gaussian distribution denoted by y_i, i.e.

$$\begin{aligned}\tilde{f}(x, y_i, \tilde{c}) = & \; c_c^T p^+ - c_d^T(p_{bat} - p^+) \\ & + c_{smg}^T u g^i \\ & + c_{peak} p_g^{ob,i} + c_{flat}(p_g^{max,i} - p_g^{min,i}) \\ & + (\tilde{c}_{buy}^T - \tilde{c}_{sell}^T) p_b^i \\ & + \tilde{c}_{sell}^T (p_d^i + p_{bat}) \\ & \text{for } i = 1, ..., N.\end{aligned} \tag{5.20}$$

The key point here is that samples only need to be generated for the net demand values with smaller sample space dimensions, yielding considerable reduction in computations. Assume that electricity prices can be modeled as

$$\tilde{c}_{buy} = c_{buy} + \zeta_1 \hat{c}_{buy}, \tag{5.21}$$

$$\tilde{c}_{sell} = c_{sell} + \zeta_2 \hat{c}_{sell}, \tag{5.22}$$

where c_{buy} and c_{sell} represent nominal prices, $\hat{c}_{buy}$ and $\hat{c}_{sell}$ are constant positive perturbations, and ζ_1 and ζ_2 are random variables which are subject to uncertainty. This chapter also models variations of electricity prices by a "Box+Polyhedral" uncertainty set denoted as U.

The only set of constraints involving the electricity prices in (5.19) are $z_i \geqslant$

$\tilde{f}(x, y_i, \tilde{c}) - \alpha \quad \forall i = 1, ..., N$. Their robust counterpart become

$$\begin{aligned}
&c_c^T p^+ - c_d^T(p_{bat} - p^+) \\
&+ c_{smg}^T u_g^i \\
&+ c_{peak} p_g^{ob,i} + c_{flat}(p_g^{max,i} - p_g^{min,i}) \\
&+ c_{buy}^T p_b^i + c_{sell}^T(p_d^i + p_{bat} - p_b^i) \\
&+ \Psi^T w_1^i + \Psi^T w_2^i + \Gamma w_3^i \\
&\leq z_i + \alpha \;\; \text{for } i = 1, ..., N,
\end{aligned} \tag{5.23}$$

where $w_1, w_2 \in \mathbb{R}^{N_h}$ and $w_3 \in \mathbb{R}$ are additional auxiliary variables needed for the robust worst case optimization (Li et al. [2011]). It is also necessary to add the following extra robust counterpart constraints to the optimization formulation

$$w_{1j}^i + w_{3j}^i \geq \hat{c}_{buy}^T p_b^i \quad \text{for} \quad j \in [1, N_h], i = 1, ..., N, \tag{5.24}$$

$$w_{2j}^i + w_{3j}^i \geq \hat{c}_{sell}^T |p_d^i + p_{bat} - p_b^i| \quad \text{for} j \in [1, N_h], i = 1, ..., N. \tag{5.25}$$

Note that constraint (5.25) contains absolute value function. In order to remove the imposed non-linearity, an equivalent robust formulation can be obtained as follows

$$\begin{aligned}
&w_{2j}^i + w_{3j}^i \geq \hat{c}_{sell}^T u^i, \\
&- u^i \leq p_d^i + p_{bat} - p_b^i \leq u^i, \\
&\text{for} \quad j \in [1, N_h], i = 1, ..., N.
\end{aligned} \tag{5.26}$$

At each time-step, the following LP optimization problem is solved

$$\begin{aligned}
\min_{\alpha,x,z_i} \quad & \left(\alpha + \frac{1}{N(1-\beta)} \sum_{i=1}^{N} z_i\right) \\
\text{subject to:} \quad & z_i \geqslant 0 \\
& + \text{the constraints in (5.9)-(5.16)} \\
& + \text{(5.23),(5.24) and (5.26).}
\end{aligned} \tag{5.27}$$

where x refers to the optimization variables consisting the following elements

$$\begin{aligned}
& p_{bat}, p^{+}, w_1, w_2 \in \mathbb{R}^{N_h}, \\
& u_g^i, p_b^i, u^i \in \mathbb{R}^{N_h} \quad (\text{for} \quad i = 1, ..., N), \\
& p_g^{max,i}, p_g^{min,i}, p_g^{ob,i}, z_i, \alpha, w_3 \in \mathbb{R} \quad (\text{for} \quad i = 1, ..., N).
\end{aligned} \tag{5.28}$$

The battery charge/discharge command is simply computed from the first sample of the optimal decision vectors p^{+} and $p_{bat} - p^{+}$.

5.3 Simulation Results

Simulations are performed on a commercial/residential setting data (with peak usage less than 24 kW) provided by Burlington Hydro Inc, with winter time of use electricity pricing, i.e., 6.2 ¢/kWh 7pm-7am, 9.2 ¢/kWh 11am-5pm, 10.8 ¢/kWh 7am-11am and 5pm-7pm Ele [2012] and selling prices, i.e., 5 ¢/kWh 7am-7pm (Independent electricy system operator, IESO). All other costs including the flattening cost, grid and battery signal smoothing costs are assumed to be small non-zero values. The battery characteristics are $E_{bat}^{min} = 0kWh$, $E_{bat}^{max} = 50kWh$, $p_{bat}^{max} = 10kW$, $P_{bat}^{loss} = 0$,

$\eta_c = 0.95$, and $\eta_d = 0.9$. The time horizon used is 24 h with variable time-step vector h=[0.5 0.5 0.5 0.5 1 1 2 2 2 2 3 3 3 3], therefore $N_h = 14$ and the rolling horizon controller updates the decisions every half an hour. The hourly electricity buy/sell costs, i.e., c_{buy} and c_{sell} are determined by the time of day, hourly buy/sell prices, and employed rolling horizon vector h. For example at midnight c_{buy}=[3.1 3.1 3.1 3.1 6.2 6.2 12.4 17 21.6 20 27.6 29.2 23.2 18.6]^T and c_{sell}=[0 0 0 0 0 0 0 5 10 10 15 15 5 0]^T.

The energy management problem is formulated and solved in two different scenarios. In the first scenario, the net electricity demand is the only uncertain parameter. A rolling horizon CVaR-based controller is proposed to model the uncertainty in demand based on a Gaussian Distribution with standard deviation of Δp_d. Here Δp_d is defined as the square root of the nominal values. The second scenario assumes that the electricity prices are exposed to uncertainty too. In this regard, two different approaches are proposed, the first one models the uncertainty in net demand and electricity prices by Gaussian distributions around their predicted nominal values while the second one models the uncertainty in electricity prices by a “Box+Polyhedral” uncertainty set. The simulations are performed over one winter month under different magnitudes of actual uncertainty in the demand as well as electricity costs. Performance of the proposed approaches are compared with their non-robust counterpart through a series of Monte-Carlo simulations in which the nominal data is perturbed by Gaussian noise with standard deviation of up to two times square root of the nominal values. Matlab is used with IBM ILOG CPLEX MILP as optimization solver using an Intel(R) Core(TM) i7-3770 CPU and 32 GB RAM to solve the optimization problem.

5.3.1 Uncertain Net Demand

A CVaR-based approach as in (5.8), in a rolling-horizon basis is adapted to model the variations in net demand signal by a Gaussian distribution with standard deviation of Δp_d around the nominal values. The number of demand samples generated to approximate cost distribution, N, and CVaR parameter β, are set to 100 and 0.9, respectively. A series of Monte-Carlo simulations is carried out to evaluate the performance of proposed robust approach and compare it to its non-robust counterpart. Therefore, monthly electricity savings for 1000 realizations of demand samples are calculated based on one set of decisions and the average cost is plotted in Figure 5.1 as a function of actual uncertainty in demand. It is worthy to note that net saving of the non-robust controller exceeds that of its robust counterpart at small levels of uncertainty in demand signal. This is the price that the robust controller has to pay for better performance at higher uncertainty values.

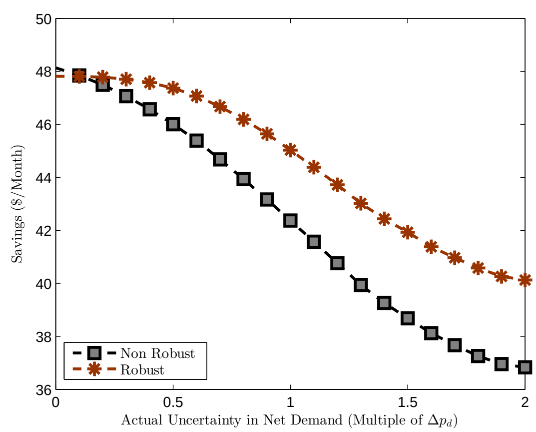

Figure 5.1: Comparison of the robust controller to its non-robust counterpart in the presence of uncertainty in demand signal. Monthly electricity savings are plotted as a function of actual uncertainty in demand.

5.3.2 Uncertain Net Demand and Electricity Prices

A similar CVaR-based approach as in (5.8) is applied to address the joint uncertainty in demand and electricity prices by modeling the uncertainty based on Gaussian distribution around their nominal values. Here, the sampling space consists of both electricity prices and net demand and hence a sufficiently large number of samples should be generated to obtain a precise approximation of the cost distribution. Since the number of constraints in the (5.8) is proportional to the number of generated samples, this impacts the computational burden of the problem. The following table shows the impact of number of samples on the optimization computational time per time-step as well as monthly cost improvement comparing to the non-robust controller.

Table 5.1: The minimum number of samples required for different cost improvements and their corresponding simulation time per time-step of the rolling horizon controller (using an Intel(R) Core(TM) i7-3770 CPU and 32 GB RAM)

Cost Improvement	CVaR	Worst-case CVaR
up to18%	$N = 200, T = 8s$	$N = 50, T = 1.3s$
$18 - 26\%$	$N = 300, T = 10s$	Not Possible

This section compares the performance of the proposed robust approaches to their non-robust counterpart for different uncertainty levels in demand and electricity prices. The first approach is simulated with $N = 300$ samples and the number of samples is reduced to $N = 50$ for the worst-case CVaR approach. Standard deviation of the Gaussian distribution used to model the variations of parameters in the first approach is set to Δp_d in net demand signal, $0.5\Delta c_{buy}$ and $0.5\Delta c_{sell}$ in the electricity prices. where, $\Delta p_d, \Delta c_{buy}, \Delta c_{sell}$ are defined as the square root of the nominal values of electricity demand, buy, and sell prices. The second approach obtains the robust counterpart formulation of the problem by tuning the parameters of "Box+Polyhedral" uncertainty set, Ψ, and Γ to 1 and two times square root of N_h, respectively. The constant positive perturbations in modeling electricity prices, i.e., $c_{\hat{buy}}$ and $c_{\hat{sell}}$, are also set to square root of the nominal electricity buy and sell prices, respectively.

The monthly savings are plotted as a function of different magnitudes of actual uncertainty in demand in Figure 5.2 (a,b,c) and actual uncertainty in costs in Figure 5.2 (d,e,f). Figure 5.2 (a,b,c) depicts the monthly saving of the controllers at three different levels of uncertainty in cost of buying electricity, i.e. Δc_{buy}, $1.5\Delta c_{buy}$, and $2\Delta c_{buy}$, respectively. The uncertainty levels are controlled by standard deviation of the Gaussian noise generated to evaluate performance of the controllers. It is worth noting that net saving of the non-robust controller exceed that of its robust counterparts at small degrees of uncertainty. This is the price that the robust controller has to pay for better performance at higher uncertainty values. Moreover, the smallest uncertainty level in demand for which the robust controllers outperform their non-robust counterpart decreases from Figure 5.2 (a) to (c) as a consequence of higher uncertainty in cost of buying electricity. Figure 5.2 (d,e,f) also presents the monthly saving of the controllers at three different levels of uncertainty in net demand, i.e. Δp_d, $1.5\Delta p_d$, and $2\Delta p_d$ in (d), (e), and (f), respectively.

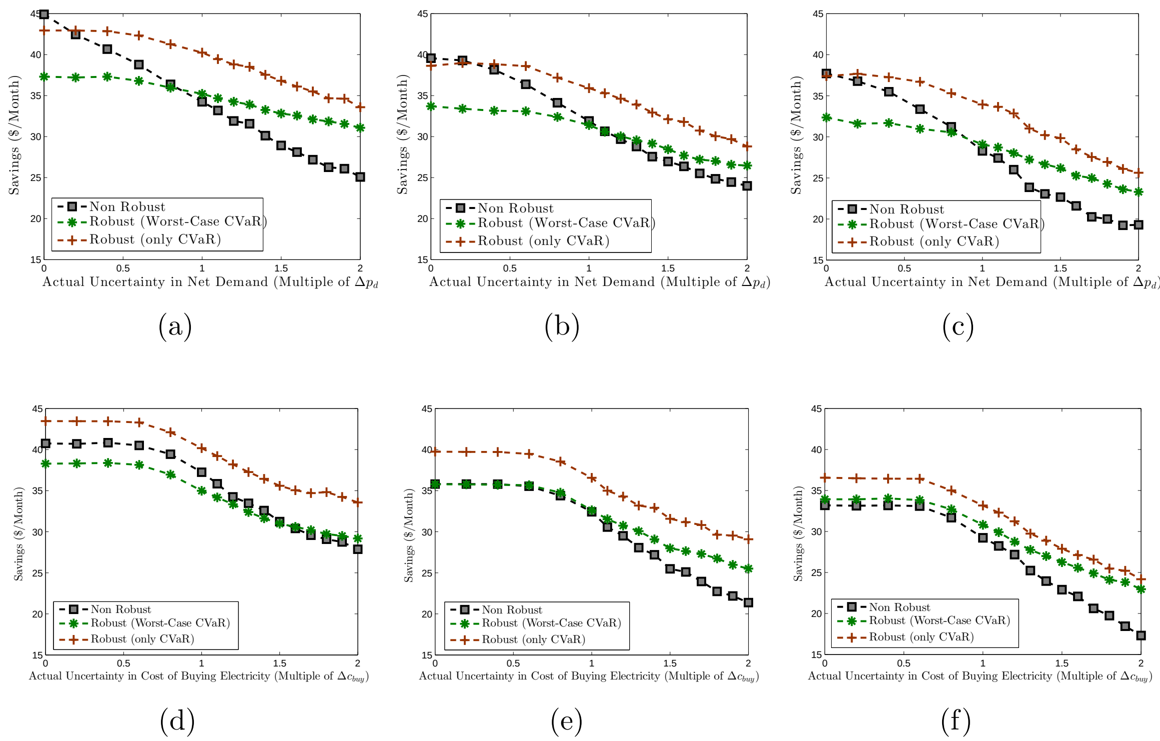

Figure 5.2: Comparison of the robust controllers to their non-robust counterparts in the presence of uncertainty in both electricity prices and demand signal. Performance of the controllers is plotted as a function of actual uncertainty in demand in (a),(b) and (c) and actual uncertainty in buying price in (d), (e) and (f) . The uncertainty level in c_{buy} is set to Δc_{buy}, $1.5\Delta c_{buy}$ and $2\Delta c_{buy}$in (a),(b) and (c), respectively. The uncertainty level in p_d is set to Δp_d, $1.5\Delta p_d$ and $2\Delta p_d$ in (d),(e) and (f).

5.3.3 Grid and Battery Signals

Figures 5.3 and 5.4 depict the grid and battery power signals associated with the proposed robust controllers under joint uncertainty of demand and electricity prices. The simulations are performed using the same commercial/residential setting as that in the previous section but with different battery specifications, i.e., $E_{bat}^{min} = 0kWh$, $E_{bat}^{max} = 15kWh$, $p_{bat}^{max} = 5kW$, $P_{bat}^{loss} = 0$, $\eta_c = 0.95$,and $\eta_d = 0.9$. The horizon vector employed, as well as electricity buy/sell prices are similar to those in the previous section. Figures 5.3 and 5.4 (a) show the grid power profile without presence of the controller. Then, the peak demand is penalized with $c_{peak} = 1$ \$/kW over a power baseline set to $p_g^{base} = 9.5$ kW and the controller attempts to keep the peak usage below that level. The grid signals associated with first and second proposed robust approaches are presented in Figures 5.3 and 5.4(b), respectively. Figures 5.3 and 5.4 (c) also demonstrate the flattening and smoothing of the grid signal with $c_{flat} = 1$ \$/kW and $c_{smg} = 0.1h$ \$/kW, respectively along with a sub-objective of battery usage with $c_c = c_d = 0.1h$ \$/kW. Note that in all the plots uncertainty in electricity prices is set to a certain level, i.e., $0.5\Delta c_{buy}$ and $0.5\Delta c_{sell}$, and the red lines in grid power profiles indicate upper and lower bounds of the grid power with $N = 1000$ different realizations of demand signal within an uncertainty interval around the nominal values. It can be seen that penalizing batteries in both approaches lead to less battery activity and consequently to non-smoothness of the grid signal.

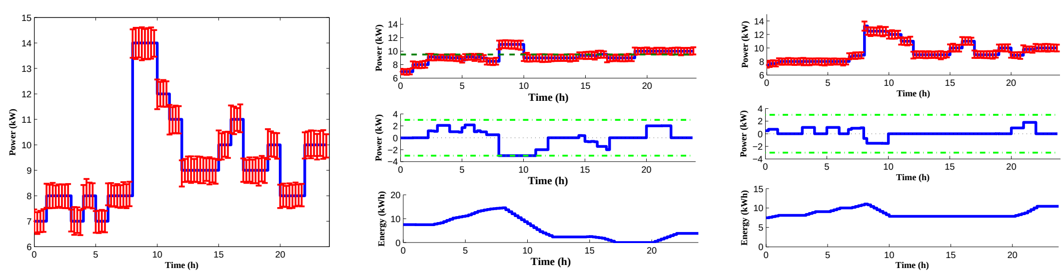

(a) (b) (c)

Figure 5.3: grid and battery signals with different sub-objectives (CVaR approach): a) net demand profile; grid power profile with no controller b) grid power profile with only flattening sub objective (top figure); battery power profile (middle figure); battery energy profile (bottom figure) c) grid power profile with grid flattening, smoothing, and battery usage sub objectives (top figure); battery power profile (middle figure); battery energy profile (bottom figure). Note that the red lines in grid power profiles indicate upper and lower envelopes of the grid power generated by $N = 1000$ different realizations of demand signal within an uncertainty interval around the nominal values.

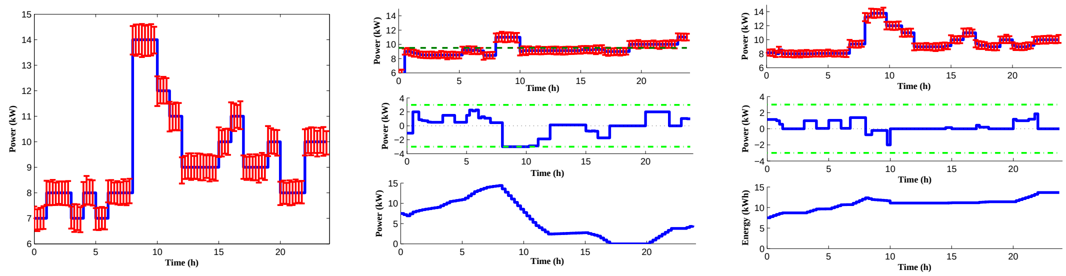

(a) (b) (c)

Figure 5.4: grid and battery signals with different sub-objectives (WCVaR approach): a) net demand profile; grid power profile with no controller b) grid power profile with peak reduction sub objective (top figure); battery power profile (middle figure); battery energy profile (bottom figure) c) grid power profile with grid flattening, smoothing, and battery usage sub objectives (top figure); battery power profile (middle figure); battery energy profile (bottom figure). Note that the red lines in grid power profiles indicate upper and lower envelopes of the grid power generated by $N = 1000$ different realizations of demand signal within an uncertainty interval around the nominal values.

Chapter 6

The Value of Coalition in a Multi-Microgrid System

This chapter studies the energy management problem of a multi-microgrid network interconnected with utility grid. In particular, a smart EMS is designed to get the most out of available resources including the generated energy and storage devices. The proposed controller benefits from a 24 hour ahead prediction of individual microgrids' net demand and makes optimal decisions in a centralized manner. In this framework, the microgrids constitute a single entity pursuing a common goal which is to keep the balance between the demand and supply of the network. In the meantime, they have the opportunity to sell their surplus resources back to the utility grid to gain extra revenue. Efficient co-operation of micro-grids increases the resiliency of the grid, reduces power loss by using local resources and transmission lines, and reduces the dependency of local grids to the utility grid. Moreover, there is a limited capacity of storage facilities in microgrids which may not be sufficient to account for the fluctuations in demand. Allowing local exchange of energy between individual microgrids may potentially compensate for the limited capacity. Consequently, this reduces the individual battery usage and prolongs the life of batteries. The rest of this chapter is organized as follows; the energy management problem is formulated in Section 6.1, Section 6.2 briefly introduces the Shapley value concept. This is followed by application of Shapley value to the energy management problem of co-operative Microgrids in Section 6.3.

6.1 Problem Formulation

Let us consider a system including N interconnected microgrids with one common point of coupling to the utility grid. The net demand power associated with each microgrid is denoted by $p_{d,i}, i = 1, .., N$ and is defined as the difference between the output power of renewable resources and the electricity usage of consumers. The same discrete-time battery model as in the Chapters 3 and 4 is employed where two different modes for the operation of batteries are considered. The first one referred to as the green zone in which battery can operate safely for an arbitrary period of time and the second one as red zone in which power rate of battery could be temporarily increased for a limited time.

Let the local variables associated to the i^{th} microgrid be concatenated in a vector denoted by $x_l^i, i = 1, ..., N$ and global decision variables of the multi-microgrid system denoted by x_g, as follows

$$\begin{aligned}
&x_l^i = p_{gc}^i, p_{rc}^i, p_{gd}^i, p_{rd}^i \in \mathbb{R}^{N_h} \quad (a)\\
&p_{bl}^i, p_{sl}^i, p_{bg}^i, p_{sg}^i \in \mathbb{R}^{N_h} \quad (b)\\
&\delta_{bs}^i, \delta_{cd}^i, \delta_r^i \in \mathbb{Z}^{N_h} \quad (c)\\
&x_g = \delta_m \in \mathbb{Z}^{N_h} \quad (d),
\end{aligned} \tag{6.1}$$

where the variables in (a) represent battery charging and discharging powers in green and red zone, respectively. The terms in (b) represent the powers which are exchanged locally among the microgrids and globally from/to the utility grid, respectively and the binary variables in (c) indicate the state of each microgrid (buying/selling, charging/discharging, and green/red zone operation). The binary vector in (d) also determines the buying/selling state of the main grid.

The energy management problem is formulated as a MILP form as follows

$$\min_{x_l, x_g} \quad \sum_i c_{buy}^i p_{bg}^i - \sum_i c_{sell}^i p_{sg}^i + \sum_i c_l p_{bl}^i \tag{6.2}$$

subject to:

$$E_{bat,i}^{min} \leq E_{bat,i} \leq E_{bat,i}^{max}, \tag{6.3}$$

$$\eta_{c,i} h^T (p_{bat}^{gc,i} + p_{bat}^{rc,i}) - \eta_{d,i}^{-1} h^T (p_{bat}^{gd,i} + p_{bat}^{rd,i}) - E_{bat}^{loss,i} h^T 1 = E_{bat}^{final,i} - E_{bat}^{0,i} \quad \forall i = 1, ..., N, \tag{6.4}$$

$$p_{bl}^i + p_{bg}^i - p_{sl}^i - p_{sg}^i + (p_{gc}^i + p_{rc}^i) - (p_{gd}^i + p_{rd}^i) = p_d^i \quad \forall i = 1, ..., N, \tag{6.5}$$

$$
\begin{aligned}
&0 \le p^i_{bat,gc} \le p^i_{bat,gcmax}\delta^i_{cd},\\
&0 \le p^i_{bat,rc} \le p^i_{bat,rcmax}\delta^i_{cd},\\
&0 \le p^i_{bat,gd} \le p^i_{bat,gdmax}(1-\delta^i_{cd}),\\
&0 \le p^i_{bat,rd} \le p^i_{bat,rdmax}(1-\delta^i_{cd}),\\
&0 \le p^i_{bat,rc} \le p^i_{bat,rcmax}\delta^i_{r},\\
&0 \le p^i_{bat,rd} \le p^i_{bat,rdmax}\delta^i_{r} \quad \forall i = 1,..,N,
\end{aligned}
\tag{6.6}
$$

$$
\begin{aligned}
&p^{gcmax,i}_{bat}\delta^i_r - p^{gcmax,i}_{bat}\left(1-\delta^i_{cd}\right) \le p^{gc,i}_{bat}\\
&p^{gdmax,i}_{bat}\delta^i_r - p^{gdmax,i}_{bat}\delta^i_{cd} \le p^{gd,i}_{bat} \quad \forall i = 1,...,N,
\end{aligned}
\tag{6.7}
$$

$$\sum_{k=j}^{j+T^{on,i}_{max_j}} h_k\delta^i_{rk} \le T^{on}_{max} \quad \forall j \in [j_{min}, j_{max}] \tag{6.8}$$

$$j_{min} = 2 - min_{h_1 l > T^{on,i}_{max}} l \in \mathcal{Z} \tag{6.9}$$

$$j_{max} = max_{\sum_{k=\gamma}^{N_h} h_k > T^{on,i}_{max}} \gamma \in \mathcal{Z} \tag{6.10}$$

$$T^{on}_{max_j} = min_{\sum_{k=j}^{j+\tau} h_k > T^{on,i}_{max}} \tau \in \mathcal{Z} \tag{6.11}$$

$$
\begin{gathered}
\delta_{r^i_{j-k-1}} - \delta_{r^i_{j-k}} \le 1 - \delta_{r^i_j}\\
\forall k \in [1, T^{off}_{min_j} - 1], \forall j \in \{[1, Nh] | T^{off}_{min_j} \ge 2\}, \forall i = 1,..,N,
\end{gathered}
\tag{6.12}
$$

$$T^{off,i}_{min_j} = min_{\sum_{k=j-r}^{j-1} h_k \ge T^{off,i}_{min}} \tau \in \mathcal{Z},\ \tau \ge 1 \tag{6.13}$$

$$
\begin{aligned}
&-\Delta p_{bat}h \le -u_{b_k}^{i} \le p_{bat_k}^{gc,i} + p_{bat_k}^{rc,i} - p_{bat_k}^{gd,i} - p_{bat_k}^{rd,i} \\
&-p_{bat_{k-1}}^{gc,i} - p_{bat_{k-1}}^{rc,i} + p_{bat_{k-1}}^{gd,i} + p_{bat_{k-1}}^{rd,i} \le u_{b_k}^{i} \le \Delta p_{bat}h \quad \forall i = 1, ..., N,
\end{aligned} \tag{6.14}
$$

$$
\begin{aligned}
-u_k^{g,i} \le & p_k^{sl,i} + p_k^{sg,i} - p_k^{bl,i} - p_k^{bg,i} + p_k^{d,i} \\
& - p_{k-1}^{sl,i} - p_{k-1}^{sg,i} + p_{k-1}^{bl,i} + p_{k-1}^{bg,i} - p_{k-1}^{d,i} \le u_k^{g,i} \quad \forall i = 1, ..., N,
\end{aligned} \tag{6.15}
$$

$$
p_{gmin}^{i} \le p_{sl}^{i} + p_{sg}^{i} - p_{bl}^{i} - p_{bg}^{i} + p_{d}^{i} \le p_{gmax}^{i} \quad \forall i = 1, .., N, \tag{6.16}
$$

$$
\begin{aligned}
&0 \le p_{bl}^{i} + p_{bg}^{i} \le p_{bl,max}^{i}\delta_{bs}^{i} \\
&0 \le p_{sl}^{i} + p_{sg}^{i} \le p_{sl,max}^{i}(1 - \delta_{bs}^{i}) \quad \forall i = 1, .., N,
\end{aligned} \tag{6.17}
$$

$$
\sum_i p_{bl}^{i} = \sum_i p_{sl}^{i} \quad \forall i = 1, ..., N, \tag{6.18}
$$

$$
\begin{aligned}
&0 \le \sum_i p_{bg}^{i} \le \delta_m p_{g,max} \\
&0 \le \sum_i p_{sg}^{i} \le (1 - \delta_m) p_{g,max},
\end{aligned} \tag{6.19}
$$

where variables with index i are local variables corresponding to the i^{th} microgrid. The optimization cost function consists of two terms; the first one is the aggregate of global electricity cost which is summed over all the microgrids and the second term is the cost associated with local transmission of energy. The inequality constraint in

(6.3) ensures that the battery energy level remains within safe limits at each time-step; here $E_{bat,i}^{min}$ and $E_{bat,i}^{max}$ denote minimum and maximum allowable battery energy levels corresponding to i^{th} microgrid. $E_{bat,i}$ is also defined as follows

$$\begin{aligned} E_{bat}^{i} =& \eta_{c,i} \sum_{j=1}^{k} h_j (p_{bat_j}^{gc,i} + p_{bat_j}^{rc,i}) - p_{bat}^{loss,i} \sum_{j=1}^{k} h_j \\ & - \eta_{d,i}^{-1} \sum_{j=1}^{k} h_j (p_{bat_j}^{gd,i} + p_{ba}^{rd,i}) + E_{bat}^{0,i}. \end{aligned} \tag{6.20}$$

The equality constraint (6.4) simply relates the battery initial energy level $E_{bat}^{0,i}$ to its final energy level $E_{bat}^{final,i}$. Equality constraint (6.5) also ensures the power balance for individual microgrids. Battery powers are also constrained by (6.6), where the scalar constants $p_{bat,gcmax}^{i}, p_{bat,rcmax}^{i}, p_{bat,gdmax}^{i}, p_{bat,rdmax}^{i}$ represent the maximum battery rates in the green and red zones, respectively. The constraint in (6.7) is added to ensure the green zone rates are used first. For safety reasons, red-zone power rates can be only activated for a maximum time of T_{max}^{on}, after which a minimum cool down time of T_{min}^{off} is needed before red-zone rates could be used again. The constraints concerning these maximum on-time and minimum off-time are presented in (6.8)-(6.13). The inequality constraint in (6.14) imposes some smoothness on the battery activities. The microgrid power profile at the point of common coupling to the utility grid is smoothened via (6.15) and the associated term in the cost; here u_g^i is an auxiliary variable corresponding to the i^{th} microgrid. The constraint (6.16) in conjunction with a term in the cost reduces the difference the microgrid minimum and maximum powers at the point of coupling to the grid, i.e., $p_g^{min^i}$ and $p_g^{max^i}$. Constraints (6.17) also limit the individual line capacities, where δ_{bs}^{i} is a binary vector indicating the buying/selling state of i^{th} microgrid, and $p_{bl,max}^{i}, p_{sl,max}^{i}$ are maximum buy/sell power rates of each line. Locally exchanged powers must also add up to zero which is taken into account by constraint (6.18). Main grid line capacity is also constrained by (6.19), where $p_{bg,max}, p_{sg,max}$ represent the maximum allowable power rates of the main grid.

6.2 Shapley Value

A co-operative game consists of N players and a characteristic function $V : 2^{[N]} \rightarrow \mathbb{R}$, which is defined on all possible coalitions of the players and generates the total cost/profit associated with each coalition. The primary idea of Shapley value theorem is to allocate players' individual share of cost, proportional to their marginal contributions. The Shapley value associated with each player is the average of marginal contributions over all the possible orders by which the players could form a complete coalition and is defined as follows

$$\Phi_i = \frac{1}{N!} \sum_R (V(P_i^R \cup \{i\}) - V(P_i^R)), \tag{6.21}$$

where R runs over all possible permutations of the players and P_i^R is the set of players preceding i in R. The denominator also indicates the total number of permutations of N players.

Let us consider the problem with $N = 3$. The possible permutations of the players numbered from 1 to N and the share of each player is listed in Table 6.1. It is noted that each permutation indicates the order in which players join the game and different sequences lead to different marginal contributions for individual players. In order to find the Shapley value associated with each player, individual coalition problems

Table 6.1: All the possible permutations and their corresponding share of players

Permutaion	Player 1	Player 2	Player 3
(1-2-3)	$V(1)$	$V(1,2) - V(1)$	$V(1,2,3) - V(1,2)$
(1-3-2)	$V(1)$	$V(1,3,2) - V(1,3)$	$V(1,3) - V(1)$
(2-1-3)	$V(2,1) - V(2)$	$V(2)$	$V(2,1,3) - V(2,1)$
(2-3-1)	$V(2,3,1) - V(2,3)$	$V(2)$	$V(2,3) - V(2)$
(3-1-2)	$V(3,1) - V(3)$	$V(3,1,2) - V(3,1)$	$V(3)$
(3-2-1)	$V(3,2,1) - V(3,2)$	$V(3,2) - V(3)$	$V(3)$

should be solved. Once the characteristic function V is obtained, the average value of each player's cost over all the permutations is the Shapley value assigned to the player.

6.3 Application of Shapley Value in Energy Management Problem of Co-operative Microgrids

In this problem, the characteristic function returns the electricity cost associated with each coalition problem. For instance, $V(1,2)$ represents the total electricity cost associated with co-operation of microgrids 1 and 2, while $V(1,2,3)$ is the electricity cost of all microgrids co-operating together. Individual coalition problems are formulated and solved by developing a rolling horizon controller which employs a 24 hour ahead prediction window of net demand power associated with each microgrid. Simulations are performed on three commercial settings (peak usage less than 10 kW) with winter time of use electricity pricing, i.e., 6.2 ¢/kWh 7pm-7am, 9.2 ¢/kWh 11am-5pm, 10.8 ¢/kWh 7am-11am and 5pm-7pm and electricity selling prices, i.e., 5 ¢/kWh 7am-7pm (Independent electricy system operator, IESO). All other costs including the flattening cost, grid and battery signal smoothing costs are set to small non-zero values. The battery characteristics are assumed to be the same for all three microgrids as following: $E_{bat}^{min} = 0kWh$, $E_{bat}^{max} = 50kWh$, $p_{bat}^{gc,max} = p_{bat}^{gd,max} = p_{bat}^{rc,max} = p_{bat}^{rd,max} = 10kW$, $T^{maxon} = T^{minoff} = 2h$, $P_{bat}^{loss} = 0$, $\eta_c = 0.95$, and $\eta_d = 0.9$. The time horizon used is 24 hour with variable time-step vector h=[0.5 0.5 0.5 0.5 1 1 2 2 2 2 3 3 3 3], therefore $N_h = 14$ and the rolling horizon controller is rolled through one week and updates the decision variables every half an hour. The hourly electricity buy/sell costs, i.e., c_{buy} and c_{sell} are determined by the time of day, hourly buy/sell prices, and employed rolling horizon vector h. For example at midnight c_{buy}=[3.1 3.1 3.1 3.1 6.2 6.2 12.4 17 21.6 20 27.6 29.2 23.2 18.6]^T and c_{sell}=[0 0 0 0 0 0 0 5 10 10 15 15 5 0]^T. Matlab is used with IBM ILOG CPLEX MILP as optimization solver using an Intel(R) Core(TM) i7-3770 CPU and 32 GB RAM to solve the optimization problem.

Individual coalition problems are solved (6.2) and the characteristic function is obtained as follows

$$V = \begin{cases} V(1) = 42.2300(\$/\text{week}) & \text{Individual operation of microgrid 1} \\ V(2) = 42.8861(\$/\text{week}) & \text{Individual operation of microgrid 2} \\ V(3) = 43.1312(\$/\text{week}) & \text{Individual operation of microgrid 3} \\ V(1,2) = 75.2724(\$/\text{week}) & \text{Coalition of microgrids 1 and 2} \\ V(1,3) = 76.1933(\$/\text{week}) & \text{Coalition of microgrids 1 and 3} \\ V(2,3) = 76.3033(\$/\text{week}) & \text{Coalition of microgrids 2 and 3} \\ V(1,2,3) = 111.7052(\$/\text{week}) & \text{Complete coalition.} \end{cases} \tag{6.22}$$

Substituting the characteristic function values from (6.22) into the Table(6.1) and averaging over all the coalitions yields the following individual costs for each player.

$$\Phi_i = \begin{cases} 36.78(\$/\text{week}) & i = 1 \\ 37.1684(\$/\text{week}) & i = 2 \\ 37.7514(\$/\text{week}) & i = 3. \end{cases} \tag{6.23}$$

This yields about 13%, 13.33% and 12.47% reduction in weekly cost of microgrids 1,2 and 3 compared to the case where each of them would operate individually, as a grid-connected microgrid.

6.3.1 Shapley Value as a Function of Infrastructure Cost

This section studies the effect of infrastructure cost in Shapley value of individual microgrids. Here, infrastructure cost, denoted by c_l, refers to the cost associated with local transmission of energy and is defined as a multiple of buying electricity prices, i.e., c_{buy}. Figure 6.1 represents the Shapley value assigned to individual microgrids as a function of c_l.

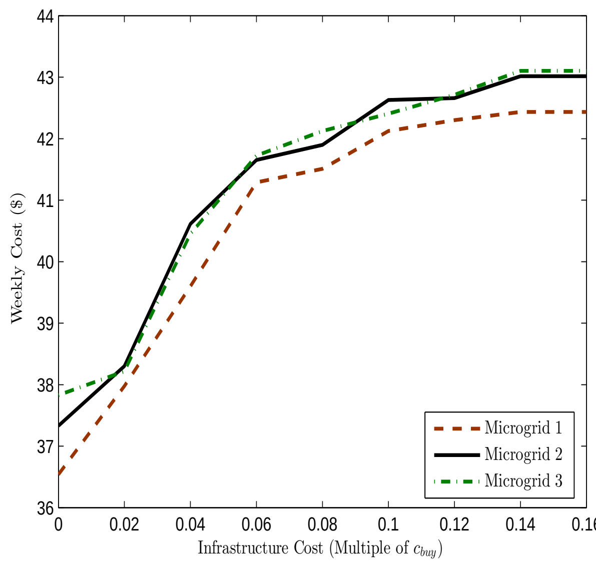

Figure 6.1: Shapley value of individual microgrids as a function of infrastructure cost

Shapley value of the microgrids grows as the infrastructure cost increases from $c_l = 0$ to $c_l = 0.16c_{buy}$. At this point, Shapley value of i^{th} microgrid converges to its individual operation cost or $V(i)$ and becomes independent of the infrastructure cost. As mentioned before, the optimization cost function denoted by J, consists of two terms as follows

$$J \triangleq \underbrace{\left(\sum_i c^i_{buy} p^i_{bg} - \sum_i c^i_{sell} p^i_{sg}\right)}_{\text{(a)}} + \underbrace{\left(\sum_i c_l p^i_{bl}\right)}_{\text{(b)}}, \tag{6.24}$$

where (6.24)(a) is the aggregate of global electricity cost and (6.24)(b) refers to the cost associated with local transmission of energy. For values of $c_l \geq 0.16 c_{buy}$, utilization of local transmission lines is not optimal any more, and therefore, each microgrid exchanges energy with its connected utility grid.

Chapter 7

Conclusion and Future Work

7.1 Conclusion

This dissertation was concerned with optimal energy/cost management of grid-connected microgrids with batteries as storage units, under uncertainty of electricity demand and prices. Two on-line MPC-based control methods were proposed to account for the uncertainty in predicted values of demand and price. The first method employed a scenario-based minimization of CVaR of the cost that assumes a Gaussian distribution for variations of both net demand and electricity prices around their predicted values. A precise approximation of CVaR requires a large number of sample scenarios, which increases the computational time of the problem. Therefore, a second method was proposed in which electricity prices were eliminated from sample space and the uncertainty was handled by a combination of worst-case robust and CVaR approaches. In particular, the uncertainty in demand and electricity prices were jointly handled by scenario-based CVaR and worst-case robust, respectively.

The cost function consists of different components including electricity usage cost, battery operation costs, and grid signal smoothing objectives. The resulting optimization problems for both methods were of MILP forms in each step of the rolling horizon. Performance of the proposed robust approaches were evaluated and compared to their non-robust counterpart through a series of Monte Carlo simulations. The simulation results indicate up to 30% and 20% improvement in the monthly electricity savings for the CVaR and the worst-case CVaR approaches compared to their non-robust counterparts, respectively.

To further reduce the complexity, a LP reformulation of the energy management problem was proposed in which binary variables are avoided. This yielded convex optimization problems that could be solved faster than their non-linear counterparts. Consequently, the elimination of binary variables makes the proposed approaches more scalable in energy management problem of multi-microgrids with larger optimization variable sets.

Finally, a game theory-based strategy was proposed to allocate individual savings of a co-operative network of microgrids interconnected with the utility grid. In the proposed approach, the energy management problem was formulated in a deterministic co-operative game theoretic framework for a group consisting of 3 connected microgrids as a single entity and the individual savings were distributed based on the Shapley value. The proposed approach yielded about 13% reduction in weekly cost of microgrids compared to the case where each of them would operate individually, as a grid-connected microgrid.

7.2 Future Work

Some possibilities for future research based on the work presented in this dissertation are discussed below.

- The formulation provided in this work can be further extended to consider other types of storage devices, such as thermal storage, flywheels, and energy capacitors.
- Electric vehicles can also be integrated with the proposed formulation in this work. This increases the overall uncertainty in the system and the robust controller should be properly modified to account for the imposed uncertainties.
- The computational burden of the proposed strategy to distribute individual savings of co-operative network of microgrids, scales up with the number of microgrids. Sampling methods can be used to approximate the Shapley value and hence make the proposed approach scalable in larger communities.

References

Annual energy outlook. `http://www.eia.gov/`, note=http://www.eia.gov/, 2014.

Alvin E Roth. *The Shapley value: essays in honor of Lloyd S. Shapley.* Cambridge University Press, 1988.

Ali Mehrizi-Sani and Reza Iravani. Potential-function based control of a microgrid in islanded and grid-connected modes. *Power systems, IEEE Transactions on*, 25(4): 1883–1891, 2010.

Thillainathan Logenthiran, Dipti Srinivasan, and David Wong. Multi-agent coordination for der in microgrid. In *Sustainable Energy Technologies, 2008. ICSET 2008. IEEE International Conference on*, pages 77–82. IEEE, 2008.

Amir H Etemadi, Edward J Davison, and Reza Iravani. A decentralized robust control strategy for multi-der microgridspart i: Fundamental concepts. *Power Delivery, IEEE Transactions on*, 27(4):1843–1853, 2012.

Yasser Abdel-Rady Ibrahim Mohamed and Ehab F El-Saadany. Adaptive decentralized droop controller to preserve power sharing stability of paralleled inverters in distributed generation microgrids. *Power Electronics, IEEE Transactions on*, 23 (6):2806–2816, 2008.

Ritwik Majumder, Arindam Ghosh, Gerard Ledwich, and Firuz Zare. Load sharing and power quality enhanced operation of a distributed microgrid. *Renewable Power Generation, IET*, 3(2):109–119, 2009.

Charles K Sao and Peter W Lehn. Control and power management of converter fed microgrids. *Power Systems, IEEE Transactions on*, 23(3):1088–1098, 2008.

Jaehong Kim, Josep M Guerrero, Pedro Rodriguez, Remus Teodorescu, and Kwanghee Nam. Mode adaptive droop control with virtual output impedances for an inverter-based flexible ac microgrid. *Power Electronics, IEEE Transactions on*, 26(3):689–701, 2011.

Qobad Shafiee, Josep M Guerrero, and Juan C Vasquez. Distributed secondary control for islanded microgridsa novel approach. *Power Electronics, IEEE Transactions on*, 29(2):1018–1031, 2014.

Mouna Rekik, Achraf Abdelkafi, and Lotfi Krichen. Synchronization of wind farm power system to utility grid under voltage and frequency variations. *International Journal of Renewable Energy Research (IJRER)*, 5(1):70–81, 2015.

Clark W Gellings. The concept of demand-side management for electric utilities. *Proceedings of the IEEE*, 73(10):1468–1470, 1985.

Sebastian Gottwalt, Wolfgang Ketter, Carsten Block, John Collins, and Christof Weinhardt. Demand side managementa simulation of household behavior under variable prices. *Energy Policy*, 39(12):8163–8174, 2011.

A-H Mohsenian-Rad, Vincent WS Wong, Juri Jatskevich, and Robert Schober. Optimal and autonomous incentive-based energy consumption scheduling algorithm for smart grid. In *Innovative Smart Grid Technologies (ISGT), 2010*, pages 1–6. IEEE, 2010a.

Amir-Hamed Mohsenian-Rad, Vincent WS Wong, Juri Jatskevich, Robert Schober, and Alberto Leon-Garcia. Autonomous demand-side management based on game-theoretic energy consumption scheduling for the future smart grid. *Smart Grid, IEEE Transactions on*, 1(3):320–331, 2010b.

Nerea Ruiz, Iñgo Cobelo, and José Oyarzabal. A direct load control model for virtual power plant management. *Power Systems, IEEE Transactions on*, 24(2):959–966, 2009.

A Gomes, CH Antunes, and AG Martins. A multiple objective approach to direct load control using an interactive evolutionary algorithm. *Power Systems, IEEE Transactions on*, 22(3):1004–1011, 2007.

DD Weers and MA Shamsedin. Testing a new direct load control power line communication system. *Power Delivery, IEEE Transactions on*, 2(3):657–660, 1987.

Karen Herter. Residential implementation of critical-peak pricing of electricity. *Energy Policy*, 35(4):2121–2130, 2007.

Chefi Triki and Antonio Violi. Dynamic pricing of electricity in retail markets. *4OR*, 7(1):21–36, 2009.

Lijun Chen, Na Li, Steven H Low, and John C Doyle. Two market models for demand response in power networks. *IEEE SmartGridComm*, 10:397–402, 2010.

Yoash Levron, Josep M Guerrero, and Yuval Beck. Optimal power flow in microgrids with energy storage. *Power Systems, IEEE Transactions on*, 28(3):3226–3234, 2013.

Faisal A Mohamed and Heikki N Koivo. Online management of microgrid with battery storage using multiobjective optimization. In *Power Engineering, Energy and Electrical Drives, 2007. POWERENG 2007. International Conference on*, pages 231–236. IEEE, 2007.

Omar Hafez and Kankar Bhattacharya. Optimal planning and design of a renewable energy based supply system for microgrids. *Renewable Energy*, 45:7–15, 2012.

Haihua Zhou, Tanmoy Bhattacharya, Duong Tran, Tuck Sing Terence Siew, and Ashwin M Khambadkone. Composite energy storage system involving battery and ultracapacitor with dynamic energy management in microgrid applications. *Power Electronics, IEEE Transactions on*, 26(3):923–930, 2011.

Edmund Handschin, F Neise, H Neumann, and R Schultz. Optimal operation of dispersed generation under uncertainty using mathematical programming. *International Journal of Electrical Power & Energy Systems*, 28(9):618–626, 2006.

Qijun Deng, Xing Gao, Hong Zhou, and Wenshan Hu. System modeling and optimization of microgrid using genetic algorithm. In *Intelligent Control and Information Processing (ICICIP), 2011 2nd International Conference on*, volume 1, pages 540–544. IEEE, 2011.

Aymen Chaouachi, Rashad M Kamel, Ridha Andoulsi, and Ken Nagasaka. Multiobjective intelligent energy management for a microgrid. *Industrial Electronics, IEEE Transactions on*, 60(4):1688–1699, 2013.

Sirus Mohammadi, Babak Mozafari, Soodabeh Solimani, and Taher Niknam. An adaptive modified firefly optimisation algorithm based on hong's point estimate method to optimal operation management in a microgrid with consideration of uncertainties. *Energy*, 51:339–348, 2013.

Diane L Peters, Abigail R Mechtenberg, John Whitefoot, and Panos Y Papalambros. Model predictive control of a microgrid with plug-in vehicles: Error modeling and the role of prediction horizon. In *ASME 2011 Dynamic Systems and Control Conference and Bath/ASME Symposium on Fluid Power and Motion Control*, pages 787–794. American Society of Mechanical Engineers, 2011.

Yi Zong, Daniel Kullmann, Anders Thavlov, Oliver Gehrke, and Henrik W Bindner. Application of model predictive control for active load management in a distributed power system with high wind penetration. *Smart Grid, IEEE Transactions On*, 3 (2):1055–1062, 2012.

Ali Hooshmand, Mohammad H Poursaeidi, Javad Mohammadpour, Heidar A Malki, and Karolos Grigoriads. Stochastic model predictive control method for microgrid management. In *Innovative Smart Grid Technologies (ISGT), 2012 IEEE PES*, pages 1–7. IEEE, 2012.

Ionela Prodan and Enrico Zio. A model predictive control framework for reliable microgrid energy management. *International Journal of Electrical Power & Energy Systems*, 61:399–409, 2014.

G Bruni, S Cordiner, V Mulone, V Rocco, and F Spagnolo. A study on the energy management in domestic micro-grids based on model predictive control strategies. *Energy Conversion and Management*, 2015.

Javier Silvente, Georgios M Kopanos, Efstratios N Pistikopoulos, and Antonio Espuña. A rolling horizon optimization framework for the simultaneous energy supply and demand planning in microgrids. *Applied Energy*, 155:485–501, 2015.

Alessandra Parisio and Luigi Glielmo. Energy efficient microgrid management using model predictive control. In *Decision and Control and European Control Conference (CDC-ECC), 2011 50th IEEE Conference on*, pages 5449–5454. IEEE, 2011.

Aharon Ben-Tal and Arkadi Nemirovski. Robust solutions of linear programming problems contaminated with uncertain data. *Mathematical programming*, 88(3): 411–424, 2000.

Pawel Malysz, Shahin Sirouspour, and Ali Emadi. An optimal energy storage control strategy for grid-connected microgrids. *Smart Grid, IEEE Transactions on*, 5(4): 1785–1796, 2014.

Yu Zhang, Nikolaos Gatsis, and Georgios B Giannakis. Robust distributed energy management for microgrids with renewables. In *Smart Grid Communications (SmartGridComm), 2012 IEEE Third International Conference on*, pages 510–515. IEEE, 2012.

Aurélie Thiele. A note on issues of over-conservatism in robust optimization with cost uncertainty. *Optimization*, 59(7):1033–1040, 2010.

R Tyrrell Rockafellar and Stanislav Uryasev. Optimization of conditional value-at-risk. *Journal of risk*, 2:21–42, 2000.

Frank J Fabozzi, Petter N Kolm, Dessislava Pachamanova, and Sergio M Focardi. *Robust portfolio optimization and management.* John Wiley & Sons, 2007.

Yu Zhang and Georgios B Giannakis. Robust optimal power flow with wind integration using conditional value-at-risk. In *Smart Grid Communications (SmartGridComm), 2013 IEEE International Conference on*, pages 654–659. IEEE, 2013.

Zhi Wu, Suyang Zhou, Jianing Li, and X-P Zhang. Real-time scheduling of residential appliances via conditional risk-at-value. *Smart Grid, IEEE Transactions on*, 5(3): 1282–1291, 2014.

Afzal Siddiqui. Optimal control of distributed energy resources and demand response under uncertainty. *Lawrence Berkeley National Laboratory*, 2010.

Sergio Bruno, Silvia Lamonaca, Giuseppe Rotondo, Ugo Stecchi, and Massimo La Scala. Unbalanced three-phase optimal power flow for smart grids. *Industrial Electronics, IEEE Transactions on*, 58(10):4504–4513, 2011.

Sumit Paudyal, Claudio Canizares, Kankar Bhattacharya, et al. Three-phase distribution opf in smart grids: Optimality versus computational burden. In *Innovative Smart Grid Technologies (ISGT Europe), 2011 2nd IEEE PES International Conference and Exhibition on*, pages 1–7. IEEE, 2011.

CM Colson and MH Nehrir. Algorithms for distributed decision-making for multi-agent microgrid power management. In *Power and Energy Society General Meeting, 2011 IEEE*, pages 1–8. IEEE, 2011.

Duong Tung Nguyen and Long Bao Le. Optimal energy management for cooperative microgrids with renewable energy resources. In *Smart Grid Communications (SmartGridComm), 2013 IEEE International Conference on*, pages 678–683. IEEE, 2013.

Muddasser Alam, Sarvapali D Ramchurn, and Alex Rogers. Cooperative energy exchange for the efficient use of energy and resources in remote communities. In *Proceedings of the 2013 international conference on Autonomous agents and multi-agent systems*, pages 731–738. International Foundation for Autonomous Agents and Multiagent Systems, 2013.

Shantanu Chakraborty, Shin Nakamura, and Toshiya Okabe. Real-time energy exchange strategy of optimally cooperative microgrids for scale-flexible distribution system. *Expert Systems with Applications*, 42(10):4643–4652, 2015.

Philippe Artzner, Freddy Delbaen, Jean-Marc Eber, and David Heath. Coherent measures of risk. *Mathematical finance*, 9(3):203–228, 1999.

Zukui Li, Ran Ding, and Christodoulos A Floudas. A comparative theoretical and computational study on robust counterpart optimization: I. robust linear optimization and robust mixed integer linear optimization. *Industrial & engineering chemistry research*, 50(18):10567–10603, 2011.

Electricity prices for residential consumers. `http://www.ieso.ca/imoweb/siteShared/options.asp?sid=ic`, note=http://www.ieso.ca/imoweb/siteShared/options.asp?sid=ic, 2012.